PROBING THE STANDARD MODEL AND BEYOND THROUGH $h o \gamma \gamma$ DECAY

LARA KRAŠOVEC

Fakulteta za matematiko in fiziko Univerza v Ljubljani

This paper explores the decay of the Higgs boson in the diphoton decay channel as a probe for the Standard Model and potential Beyond Standard Model phenomena. An outline of the Higgs mechanism in the context of the electroweak theory is presented, followed by the computation of the SM Higgs boson decay width using dimensional regularization and Passarino-Veltman reduction implemented through Package-X. Additional contributions of charged scalars arising in various BSM theories are considered. Using recent experimental measurement of the diphoton signal strength, constraints are placed on the parameters of singly and doubly charged Higgses. The fit shows a mild preference for nonzero negative couplings at the 1σ level, which is not statistically significant.

RAZISKOVANJE (ONKRAJ) STANDARDNEGA MODELA PREK RAZPADA $h \to \gamma \gamma$

Članek obravnava razpad Higgsovega bozona v dva fotona in njegovo vlogo pri iskanju procesov onkraj Standardnega modela. Predstavljen je Higgsov mehanizem v kontekstu elektrošibke teorije. Sledi izračun razpadne širine Higgsovega bozona v Standardnem modelu z uporabo Package-X, ki sloni na dimenzacijski regularizaciji in Passarino-Veltman redukciji. Dodatno so obravnavani prispevki procesov, ki vključujejo nabite skalarje, prisotne v razširitvah Standardnega modela. Na podlagi eksperimentalnih podatkov so določene omejitve parametrov enojno in dvojno nabitih skalarjev, pri čemer je opazna težnja k negativnim sklopitvam pri 1σ , kar pa ni statistično signifikantno.

Acknowledgements

I would like to sincerely thank my advisor prof. dr. Miha Nemevšek and my co-advisor dr. Jonathan Kriewald for their theoretical insight and patience, as well as for their suggestions regarding the structure of the paper. Their imput improved both its technical quality and its readability.

1 Introduction

The development of the quantum field theory in the first half of the 20th century led to the formulation of a remarkably successful description of the interactions among the elementary particles – the Standard model (SM). The gradual building of this theoretical framework spanned more than three decades, with the need for stringent tests of its predictions being to this day the main objective of many collaborations in experimental particle physics.

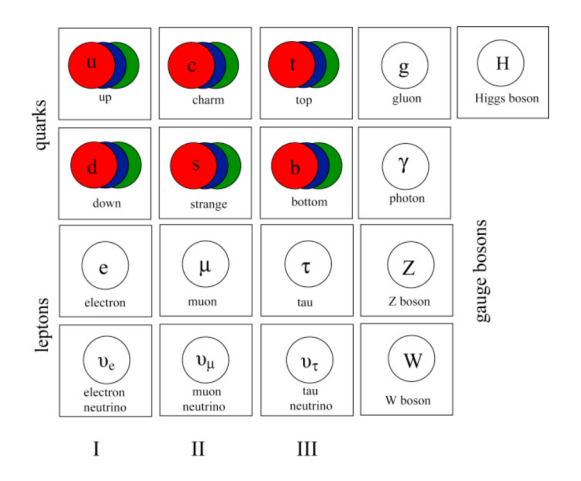
The theoretical description of the weak force and its unification with electromagnetism was perhaps the most demanding, both because of the parity-violating nature of the weak interaction as well as due to the mathematical challenge of formulating a theory with massive vector bosons. The solution – the celebrated *Higgs mechanism* – was proposed in 1964 by Higgs [1], Brout and Englert [2], as well as Guralnik, Hagel and Kibble [3]. In 1967, this enabled Weinberg [4] and Salam [5], who continued the work of Glashow [6], to develop the *electroweak theory*, which was in 1971 proved by t'Hooft and Veltman [7] to be renormalizable, that is, giving finite results.

Besides the W and Z bosons, discovered in 1983, the electroweak theory predicted the existence of a neutral scalar particle – the $Higgs\ boson$, which prompted the construction of CERN's Large Hadron Collider (LHC). Its discovery was announced in 2012 [8, 9], thus establishing the SM as the fundamental theory of nature. The particle content of the SM is presented in Figure 1.

© © 2025 The Author(s). Original content from this work may be used under the terms of the Creative Commons Attribution 4.0 licence.

Despite its success, the Standard model fails to explain certain observations, such as the presence of dark matter, and predicts massless neutrinos, while experiments have shown evidence for non-zero masses. Moreover, some theoretical considerations hint at the need for the unification of the forces. It is generally believed that the SM is not the final theory of fundamental particles and there exists physics beyond it. There is a plethora of theoretical frameworks that address the difficulties mentioned earlier, which usually requires the introduction of new particles. These could be detected directly by observing their decays or indirectly by noticing their effects in scatterings or decays of known SM particles. In particular, some of the theorised beyond Standard model (BSM) particles could couple to the SM Higgs boson and contribute to its decay width.

Figure 1: The Standard model of particle physics describes fermions – spin 1/2 particles that make up matter – and bosons with integer spin. Fermions are divided into three generations of quarks which come in three colors and three generations of leptons [10]. Gauge bosons are vector (spin 1) particles that mediate interactions. An important piece of the puzzle that was added to the model after having been experimentally confirmed in 2012 is the scalar (spin 0) Higgs boson [8, 9].



Among other decay modes, the Higgs boson can decay to two photons through a loop-induced process. Despite its small branching ratio, the diphoton decay channel played an important role in the Higgs boson detection and has been crucial in the ensuing precision measurements, alongside the 'golden' four-lepton channel. Both have low backgrounds and allow for excellent resolution [11].

The diphoton decay channel is of significant importance not only because of its clean signature but also due to its sensitivity to BSM corrections. As the process does not occur at tree level it is possible to consider theorised new particles entering the loop and having observable consequences.

We begin with a brief introduction to some key aspects of group theory, quantum field theory and gauge fields, followed by an explicit theoretical discussion of the electroweak theory in the Standard model. After listing the relevant Feynman rules, we use those to obtain the SM prediction for the $h \to \gamma \gamma$ decay width. Following a slight experimental aside, we compute hypothetical contributions of charged scalars to the decay width and use experimental data to constrain the parameters of such BSM models. For readers interested in a more rigorous treatment of the electroweak theory, as well as the technical details of the decay width computation, these are available in the appendices.

2 Gauge symmetries

2.1 Brief overview of symmetries and groups

The symmetry of a particular system can be considered in the context of its symmetry group – the group of all transformations under which the system remains invariant. Since symmetries play a key role in describing high-energy physics phenomena, we will rely on some basics of group theory throughout this article. In our ensuing discussion we will limit ourselves to *continuous symmetries*, which are described by Lie groups, parametrized by a continuous parameter. A general transformation of a field χ under a Lie group can be written as $\chi \to \chi' = e^{i\epsilon_a T^a} \chi$, where ε_a are the continuous group parameters and T^a are the generators. The latter form a basis of the Lie algebra of the group

and satisfy the commutation relation: $[T^a, T^b] = i f_{abc} T^c$, with f_{abc} as the structure constants [12].

Global and local symmetries. In the case of local symmetries, the parameters are functions of coordinates; $\varepsilon = \varepsilon(x^{\mu})$, whereas global symmetries act the same at each spacetime point; $\varepsilon \neq \varepsilon(x^{\mu})$ [13].

Abelian and non-abelian groups. For a group to be considered abelian all of its elements must commute. One example we will encounter is the group of phase rotations U(1) which transform a field χ as: $\chi \to e^{i\varepsilon}\chi$, where ε is a real continuous parameter. Elements of non-abelian groups are in general non-commutative. Such is the special unitary group SU(n), which is the group of all $n \times n$ unitary matrices with determinant 1 (hence 'special'). The group SU(n) has $n^2 - 1$ generators for reasons related to the unitarity constraint [12].

Group representations. Transformation under a given symmetry group can be written as $\chi' = U\chi$, where U is a matrix realization of a group element acting on χ and is called a representation of the group [13]. Different fields χ can transform under different representations of the same group. For example, the *adjoint representation* tells us how the group acts on its own Lie algebra. The fundamental representation, on the other hand, is the most basic irreducible representation. For SU(n) it is n-dimensional and acts on n-dimensional complex vectors [12].

2.2 Quantum field theory and the Standard model

Our main focus will be on the interactions among elementary particles. These are described by their respective quantum fields and treated in the context of quantum field theory (QFT).

A system is described by its Lagrangian density, which is in a field theory a function of fields and their derivatives: $\mathcal{L}(\chi, \partial_{\mu}\chi)$. Here four space-time derivatives are combined into $\partial_{\mu} = (\partial_t, \vec{\nabla})$ to allow for Lorentz invariance of the theory. Corresponding equations of motion are derived by varying the action $S = \int dx^4 \mathcal{L}$.

The particles in the Standard model (SM) are presented in Figure 1. Lagrangians of non-interacting scalar (ϕ) , fermion (ψ) and vector (B_{μ}) fields are listed below:

•
$$\mathbb{R} \text{ scalar}: \quad \mathcal{L} = \frac{1}{2} \left(\partial_{\mu} \phi \right) \left(\partial^{\mu} \phi \right) - \frac{1}{2} m^{2} \phi \phi ,$$
 • $\mathbb{R} \text{ vector}: \quad \mathcal{L} = -\frac{1}{4} F_{\mu\nu} F^{\mu\nu} + \frac{1}{2} m^{2} B^{\mu} B_{\mu} ,$
• $\mathbb{C} \text{ scalar}: \quad \mathcal{L} = \left(\partial_{\mu} \phi \right) \left(\partial^{\mu} \phi^{*} \right) - m^{2} \phi \phi^{*} ,$ • fermion: $\mathcal{L} = \bar{\psi} i \partial \!\!\!/ \psi - m \bar{\psi} \psi .$

We introduced the Feynman slash notation: $\partial = \gamma^{\mu} \partial_{\mu}$, where γ^{μ} are the Dirac γ matrices. The field strength tensor $F_{\mu\nu}$ will be defined in the next section. The terms quadratic in fields which include derivatives are *kinetic* and those that do not are the *mass terms*. These are the free field Lagrangians and do not contain interaction terms.

Here, fields were introduced as complex-valued functions of space-time coordinates, following the classical field theory approach. In the full quantum field theory, these classical fields are promoted to operators with canonical commutation relations, and particles emerge as discrete excitations of these quantized fields with specific energy eigenvalues.

2.3 Introduction to gauge theories

In the Standard model, every fundamental interaction arises from requiring that the Lagrangian remains invariant under local transformations. This gauge invariance can only be achieved by the introduction of spin-1 gauge fields, which mediate the forces. Without gauge invariance, a theory becomes nonrenormalizable [14], meaning the infinities which arise in the calculations cannot be

cancelled out, thereby stripping the theory of its consistency.

Abelian gauge theories: U(1) example. Let us first consider a theory of a free complex scalar field ϕ . It is described by the Lagrangian given in (1), which is manifestly invariant under global U(1) transformations. It is not invariant under local U(1) transformations, however, as derivatives in the first term act on the spacetime-dependent parameter $\varepsilon(x^{\mu})$. To achieve gauge invariance we introduce a gauge-covariant derivative \mathcal{D}_{μ} , defined by:

$$\mathcal{D}_{\mu}\phi = (\partial_{\mu} - ieA_{\mu})\phi, \qquad (2)$$

where A_{μ} is a gauge field which transforms as: $A_{\mu} \to A_{\mu} + \frac{1}{e} \partial_{\mu} \varepsilon \,.$

$$A_{\mu} \to A_{\mu} + \frac{1}{e} \partial_{\mu} \varepsilon$$
 (3)

After promoting the derivatives ∂_{μ} in the Lagrangian (9) to the gauge-covariant derivative defined earlier, all of the terms that arise because of the spacetime-dependence of ε cancel out and such a Lagrangian has a local U(1) invariance. In addition, the theory now contains a gauge field A_{μ} , which is coupled to the scalar field. We have therefore generated interactions.

Non-abelian gauge theories: SU(2) example. The concept of gauge invariance can be extended to non-abelian gauge groups. If a complex scalar field ϕ transforms under a certain representation of SU(2) as $\phi(x) \to \omega(x)\phi(x)$, then gauge invariance of the Lagrangian is again achieved by introducing the covariant derivative like we did in (2), except that now A_{μ} transforms as $A_{\mu} \to A'_{\mu} = \omega A_{\mu} \omega^{-1} + \omega \partial_{\mu} \omega^{-1}$ and is matrix-valued. It can then be written in the basis of the group generators in the appropriate representation: $A_{\mu} = \sum_{a} T^{a} A^{a}_{\mu}$ [13], where we denoted by A^{a}_{μ} a number-valued field associated with the generator T^{a} . In all future instances the sum over repeated indices will be omitted. For the fundamental representation of SU(2), the generators are normalized Pauli matrices: $T^{a} = \sigma^{a}/2$, which means we can write the covariant derivative as:

$$\mathcal{D}_{\mu}\phi = \left(\partial_{\mu} - ig\frac{\sigma^{a}}{2}A_{\mu}^{a}\right)\phi. \tag{4}$$

When introducing a new field into the theory we must also include its kinetic term, written as:

$$\mathcal{L}_{\text{gauge, kinetic}} = -\frac{1}{4} F_{\mu\nu}^a F_a^{\mu\nu}, \qquad F_{\mu\nu}^a = \partial_{\mu} A_{\nu}^a - \partial_{\nu} A_{\mu}^a + g f_{abc} A_{\mu}^b A_{\nu}^c.$$
 (5)

In the case of abelian gauge groups, the structural constants are zero, hence the third term in the definition of $F_{\mu\nu}$ vanishes. For non-abelian gauge fields, however, the presence of this term leads to triple and quartic self-interactions of the fields. For SU(2), the structural constants f_{abc} are the components of the Levi-Civita symbol ε_{abc} .

Moreover, a mass term for the gauge fields is prohibited by the gauge invariance. Considering again the abelian example, a mass term is not invariant under the U(1) transformations:

$$\frac{1}{2}m_A^2 A_\mu A^\mu \longrightarrow \frac{1}{2}m_A^2 \left(A_\mu + \frac{1}{e}\partial_\mu \varepsilon\right) \left(A^\mu + \frac{1}{e}\partial^\mu \varepsilon\right) \neq \frac{1}{2}m_A^2 A_\mu A^\mu \,, \tag{6}$$

and therefore cannot be included *ad hoc* in a gauge-invariant Lagrangian. However, some of the gauge bosons in the Standard model are massive. A fascinating solution to this problem lies in the spontaneous breaking of the gauge symmetry through the Higgs mechanism.

2.4 Spontaneous symmetry breaking (SSB)

Consider a Lagrangian, invariant under some symmetry group, with a kinetic part T and a potential V: $\mathcal{L} = T - V$. If terms that violate the invariance are added to the Lagrangian, the symmetry becomes only approximate. This is known as explicit breaking.

On the other hand, if \mathcal{L} is invariant under the symmetry and the minimum of the potential, i.e. the vacuum, does not respect the symmetry of the Lagrangian, its symmetry group can be broken spontaneously by expanding \mathcal{L} around the minimum. According to the Goldstone theorem, if the spontaneously broken symmetry of a Lorentz-invariant theory is continuous and global, this results in the appearance of massless scalar states in the spectrum of the theory – the Nambu-Goldstone bosons (NGBs) [15], one for each spontaneously broken generator. An example of a spontaneous breaking of a global symmetry is available in the Appendix. If the spontaneously broken symmetry is local, however, the NGBs can be thought of as absorbed by the gauge bosons, which as a result acquire mass [12]. This mathematical procedure is called the Higgs mechanism and will be discussed in the following section.

3 Electroweak theory in the Standard model

We are now set to construct the proper electroweak theory of the Standard model. As the name implies, electromagnetic and weak interactions are treated within the same unified theoretical framework. In order to ensure its renormalizability, we require a certain gauge invariance of the theory, which will have to be spontaneously broken to generate the masses of the weak bosons W^{\pm} and Z.

3.1 Gauge group of the electroweak theory

For simplicity we will consider only the first generation of leptons: left- and right-handed electrons, e_L, e_R , and the left-handed electron neutrino, ν_L . The interactions of these particles are governed by the gauge group of the theory. In order to accommodate both self-interacting W^{\pm}_{μ} bosons as well as the photon field A_{μ} , the gauge group must consist of a non-abelian and an abelian part. A valid choice is $SU(2) \otimes U(1)$, which has 3+1=4 generators. The explicit connection between the group generators and the vector boson fields is not obvious and is shown in the Theoretical Appendix 7.

Since the weak interaction violates parity, fermion fields of different chirality must transform under different representations of SU(2). We therefore take the left-handed leptons to form a SU(2) doublet and treat the right-handed one as an SU(2) singlet:

$$\begin{pmatrix} \nu_L \\ e_L \end{pmatrix}, \quad e_R.$$

From now on, the SU(2) part of the gauge group will be denoted as $SU(2)_L$ to convey this information. Transformations of the fields under U(1) are indicated by their U(1) quantum number – weak hypercharge Y. The gauge group of the electroweak theory is then written as:

$$SU(2)_L \otimes U(1)_Y$$
. (7)

3.2 Spontaneous symmetry breaking: the Higgs mechanism

Besides fermions and gauge fields we want the theory to also include scalar fields with a potential that allows for SSB (see Appendix 7). More specifically, we need to break both the $SU(2)_L$ and $U(1)_Y$ parts of the gauge group. This is achieved by introducing scalars that transform non-trivially under both groups. The simplest option is a doublet of two complex scalar fields ϕ_1 and ϕ_2 :

$$\phi = \begin{pmatrix} \phi_1 \\ \phi_2 \end{pmatrix} \,, \tag{8}$$

with hypercharge $Y_{\phi} = 1/2$, as derived in Appendix 7. We now write the gauge-invariant Lagrangian for the scalar part of the theory:

$$\mathcal{L}_{\text{Higgs}} = (\mathcal{D}_{\mu}\phi)^{\dagger} (\mathcal{D}^{\mu}\phi) - V(\phi), \qquad V(\phi) = -\mu^{2}\phi^{\dagger}\phi + \lambda \left(\phi^{\dagger}\phi\right)^{2}, \qquad \mu^{2}, \lambda > 0.$$
 (9)

It follows from Section 2.3 that gauge invariance is ensured by defining the covariant derivative as:

$$\mathcal{D}_{\mu}\phi = \left(\partial_{\mu} + igT^{a}W_{\mu}^{a} + ig'Y_{\phi}B_{\mu}\right)\phi, \tag{10}$$

where T^a are the three generators of $SU(2)_L$, W^a_μ are the real number-valued gauge fields associated with them, while B_μ corresponds to the $U(1)_Y$ gauge field. We introduced two coupling constants, g and g', as well as the $U(1)_Y$ quantum number of the scalar doublet, Y_ϕ . Differentiating $V(\phi)$ with respect to ϕ_1 and ϕ_2 , we obtain the following condition for the possible minima:

$$|\phi_1|^2 + |\phi_2|^2 = \frac{1}{2}v^2$$
, $v^2 = \frac{\mu^2}{\lambda}$. (11)

Choosing one of the solutions and expanding the scalar fields around it, we get:

$$\langle \phi \rangle = \begin{pmatrix} \langle \phi_1 \rangle \\ \langle \phi_2 \rangle \end{pmatrix} = \begin{pmatrix} 0 \\ \frac{v}{\sqrt{2}} \end{pmatrix} \longrightarrow \phi = \langle \phi \rangle + \begin{pmatrix} w^+ \\ \frac{1}{\sqrt{2}} (h + iz) \end{pmatrix} = \begin{pmatrix} w^+ \\ \frac{1}{\sqrt{2}} (v + h + iz) \end{pmatrix}, \quad (12)$$

where w^+ is the perturbation around the vev of ϕ_1 , while $(h+iz)/\sqrt{2}$ is the perturbation around the vev of ϕ_2 , split into its real and imaginary parts denoted by relatively suggestive notation. Fields z, w^+ and its complex conjugate w^- are the would-be Goldstone bosons [16], which are unphysical and can be shown to be absorbed by the massive gauge bosons by fixing an appropriate gauge [12]. The theory predicts the existence of a massive neutral scalar h – the Higgs boson. After inserting the expansion of ϕ as defined in Equation (12) into the Lagrangian (9), its initial symmetry is spontaneously broken and we obtain appropriate mass terms for the weak bosons. The interesting intricacies of the electroweak SSB, including the derivation of the mass terms and the pattern of the SSB, are discussed in the Theoretical Appendix 7, which the reader is kindly encouraged to consider.

3.3 Feynman rules for the electroweak theory

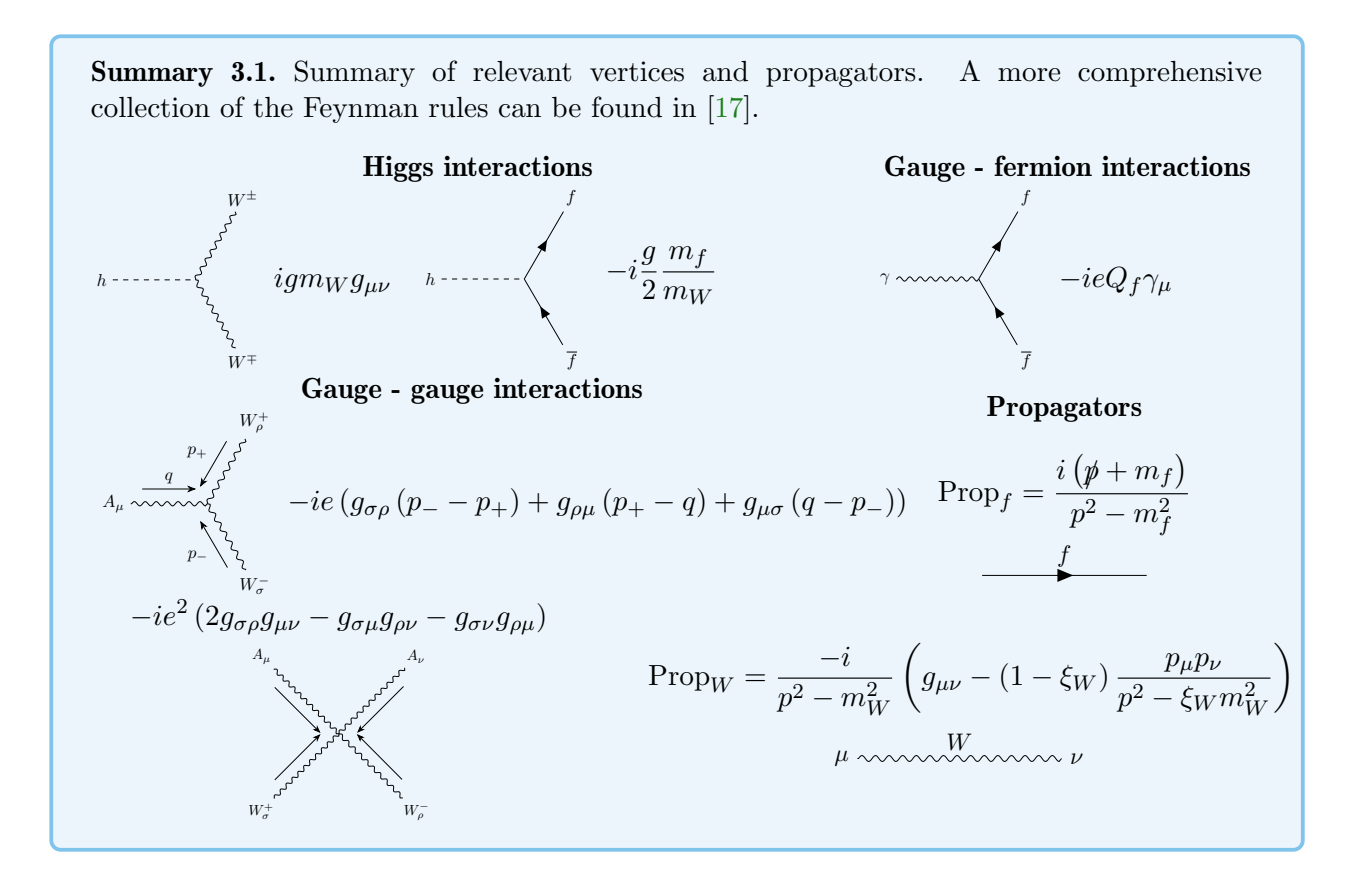
So far, we have only discussed the first term of the electroweak Lagrangian, \mathcal{L}_{Higgs} , given in Equation (9). The entire electroweak theory, however, can be separated into the following sectors [17]:

$$\mathcal{L}_{\text{SM}}^{\text{EW}} = \mathcal{L}_{\text{Higgs}} + \mathcal{L}_{\text{gauge}}^{\text{pure}} + \mathcal{L}_{\text{fermion}}^{\text{pure}} + \mathcal{L}_{\text{Yukawa}} + \mathcal{L}_{\text{gf}} + \mathcal{L}_{\text{ghost}}.$$
 (13)

We are mainly concerned with the calculation of the $h \to \gamma \gamma$ decay. The electroweak Lagrangian contains instructions for that in the form of particle couplings and propagators – the *Feynman rules*, which are collected in Summary 3.1. Some further remarks on their derivation are provided in Appendix 7.

When quantizing gauge theories, redundant field configurations stemming from the gauge invariance must be removed by introducing the gauge-fixing terms [12]. This allows us to properly derive the propagators, which consequently depend on an arbitrary gauge parameter ξ , as seen in 3.1. Our calculation of $h \to \gamma \gamma$ decay will be performed in the *unitary gauge*, obtained by setting $\xi \to \infty$. In this limit, the unphysical degrees of freedom, such as the would-be Goldstones, are eliminated, which simplifies the calculation significantly. The W boson propagator defined in 3.1 then becomes:

$$Prop_W = \frac{-i}{p^2 - m_W^2} \left(g_{\mu\nu} - \frac{p_{\mu}p_{\nu}}{m_W^2} \right). \tag{14}$$



4 Testing the electroweak theory

4.1 Experimental measurement

Since its detection in 2012, the properties of the Higgs boson have been studied extensively by ATLAS and CMS Collaborations [18, 11]. Higges are produced in proton-proton collisions predominantly through gluon fusion involving a top quark loop. The SM lifetime is $\tau_h \approx 1.6 \cdot 10^{-22}$ s, meaning the Higgs boson decays rapidly into lighter states. The branching fractions of the decay channels are visualized in figure 2b. Although the $h \to \gamma \gamma$ is a relatively rare decay, it was one of the main discovery channels, the other being the 'golden' four-lepton channel, with an even smaller branching ratio. The reason lies in their extremely clean signatures with low background.

Unlike for the dominant $b\bar{b}$ channel with overwhelming quark background from QCD processes, the only background for the diphoton channel comes from quark annihilation, gluon-gluon fusion and jet or particle misidentification. This background forms a smooth distribution which can be modelled and taken into account during data analysis. The photons are detected in *electromagnetic calorimeters*, where they produce electromagnetic showers after interacting with the detector material.

The invariant mass of the two photons is then calculated from the measured energies and their directions of detection. The photons originating from Higgs boson decays create a bump in the background spectrum, as seen in Figure 2a. This peak is centered at the mass of the decaying particle and is approximately Gaussian due to the detector resolution effects, which completely mask the true Breit-Wigner resonance shape. Current experimental value of the Higgs boson mass obtained from such measurements is $m_h = 125.38 \pm 0.14$ GeV ($m_h = 125.17 \pm 0.14$ GeV) as found by CMS [11] (ATLAS [18]).

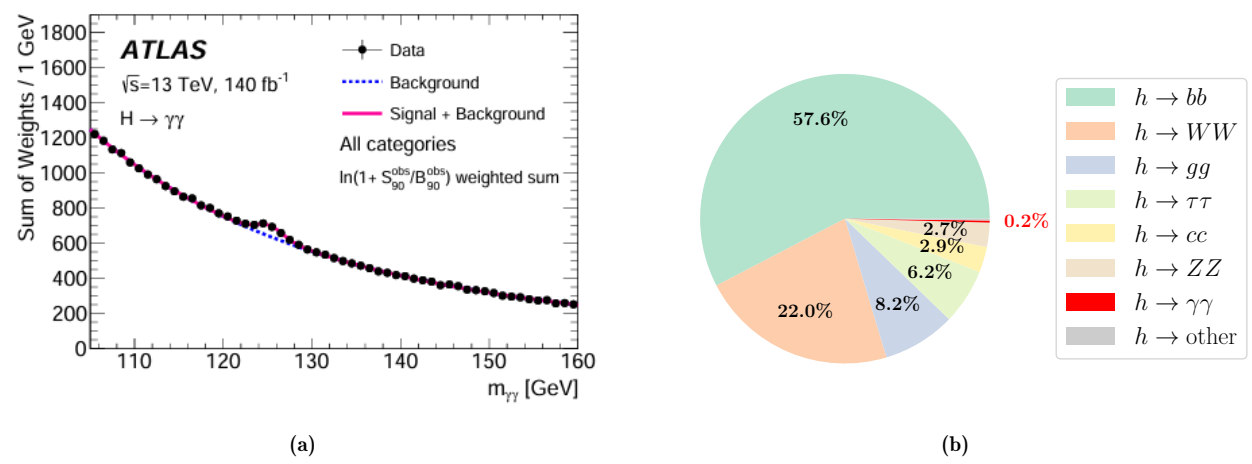


Figure 2: a) Diphoton invariant mass distribution with background (dotted blue line) and fit (red line). Source: [18]. b) Branching fractions of the h decay channels. Data was obtained from [19].

4.2 Standard model predictions for $h \rightarrow \gamma \gamma$ decay width

The Higgs boson cannot couple to photons directly. Since it has zero electric charge, this can be understood from electrodynamics. Fittingly, there are no h- γ interaction terms in the electroweak Lagrangian. Moreover, the Higgs boson only couples to massive particles, and γ is massless.

The $h \to \gamma \gamma$ decay therefore occurs at higher orders of the perturbative expansion, with the lowest non-trivial order being at one-loop. Particles that can enter in the loop must be charged (coupling to γ) and massive (coupling to h). In the SM, that leaves us with charged fermions and the W boson. Higgs coupling is proportional to the mass of a particle, so we can assume the main contributors will be the top quark and the W, with masses $m_t \approx 173$ GeV and $m_W \approx 80$ GeV [19].

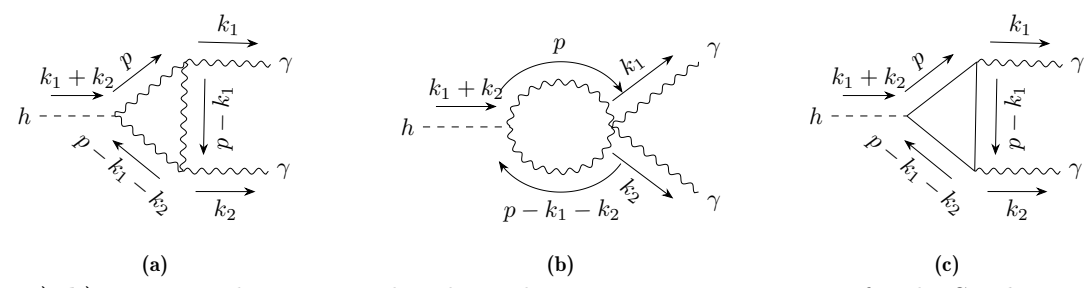


Figure 3: a), b) Feynman diagrams with indicated momentum assignments for the SM $h \to \gamma \gamma$ decay with the W boson in the loop. We refer to the one on the left as the *triangle* diagram and the one with the quartic vertex as the *bubble*. c) Feynman diagram with a charged fermion in the loop.

In unitary gauge, there are two Feynman diagrams involving the W boson and one diagram corresponding to the fermion loop which contribute to the SM decay width. They are presented in Figure 3. We can use the Feynman rules listed in Section 3.3 to write down the appropriate amplitudes. However, there are a few other considerations to be made. The particles in the loop are virtual or off-shell, which means they do not satisfy the classical equations of motion and can have arbitrary momenta, as long as energy and momentum are conserved at each vertex. We must therefore integrate over all possible loop momenta p. In general, such loop integrals are not finite and need to be dealt with using a certain regularization method. Here, we employ dimensional regularization, which means promoting a 4-dimensional integral to d-dimensions and evaluating it, after which we set $d = 4 - \varepsilon$, where $\varepsilon \to 0$. This helps us to isolate the divergent terms, which cancel out after considering all of the contributing diagrams, since the observables must be finite. For additional comments on renormalization, see Appendix 7.1.

Evaluating the loop integrals is not exactly trivial. The results were computed in Mathematica

using Package-X [20], with the corresponding code available in Appendix 8.1. In the present section we outline the final results, which match those in the literature [21].

Adding together the expressions for the W and the fermion amplitudes and summing over all possible fermion states in the loop leads to the total Standard model amplitude for the $h \to \gamma\gamma$ decay at one-loop order, which can be compactly written as:

$$\mathcal{M}_{SM} = \mathcal{M}_W + \sum_f \mathcal{M}_f = \frac{e^2 g}{(4\pi)^2 m_W} F_{SM} \left(k_1 \cdot k_2 g^{\mu\nu} - k_1^{\nu} k_2^{\mu} \right) \varepsilon_{\mu}(k_1) \varepsilon_{\nu}(k_2) \,. \tag{15}$$

We defined $F_{\rm SM}$ as $F_{\rm SM} = F_W + \sum_f N_f Q_f^2 F_f$ with

$$F_W = 2 + 3\beta_W + 3(2\beta_W - \beta_W^2) f(\beta_W)$$
 and $F_f = -2\beta_f (1 + (1 - \beta_f)f(\beta_f))$, $\beta_i = \frac{4m_i^2}{m_i^2}$. (16)

Here Q_f is the electric charge of the fermion in units of e and N_f is the *color factor*, which is 1 for leptons and 3 for quarks. The function $f(\beta)$ is defined as:

$$f(\beta) = \begin{cases} \arcsin^2 \left(\beta^{-1/2}\right), & \beta \ge 1, \\ -\frac{1}{4} \left(\ln \frac{1+\sqrt{1-\beta}}{1-\sqrt{1-\beta}} - i\pi\right)^2, & \beta < 1. \end{cases}$$

Using the masses m_h , m_t and m_W given earlier, and knowing $N_t = 3$ and $Q_t = 2/3$ for the top quark, we can compute the dimensionless constants F_W and F_t :

$$F_W \approx 8.3$$
, $F_t \approx -1.4 \rightarrow N_t Q_t^2 F_t \approx -1.8$. (17)

The top quark therefore interferes destructively with the W loop, which gives the dominant contribution, as $F_W > N_t Q_t^2 |F_t|$. After some algebra, provided in Appendix 8.1, we arrive at the SM prediction for the $h \to \gamma \gamma$ decay width at one-loop:

$$\left| \Gamma_{h \to \gamma \gamma}^{\text{SM}} = \frac{m_h^3 G_F}{8\sqrt{2}\pi} \left(\frac{\alpha}{4\pi} \right)^2 |F_{\text{SM}}|^2 \right|, \tag{18}$$

where G_F and α are the Fermi constant the fine-structure constant, which are defined as:

$$\frac{8G_F}{\sqrt{2}} = \frac{g^2}{m_W^2} \quad \text{and} \quad \alpha = \frac{e^2}{4\pi} \,. \tag{19}$$

Additional terms in the perturbative expansion would be surpressed by higher powers of the coupling constants. Expression (18) agrees with the result in [21]. We note that the divergencies cancelled out and the observable Γ is indeed finite.

5 Search for the evidence of physics beyond the Standard model

Since it occurs at one-loop order, the $h \to \gamma \gamma$ decay is especially interesting as a probe for BSM phenomena. Many SM extensions predict the existence of additional particles that would couple to both the Higgs boson and the photon, which means they would contribute to the process as virtual loop states. Such are for example charged Higgs bosons, which are present in but not limited to the following models: Type-II See-Saw [22], Left-Right Symmetric Model (LRSM) [23], Minimal Supersymmetric Standard Model (MSSM) [24]. Typically, these additional scalars are doubly charged at most. For the purposes of this paper, we therefore consider the contributions of arbitrary charged scalars $\Delta^{+(+)}$ and modify our previous results accordingly.

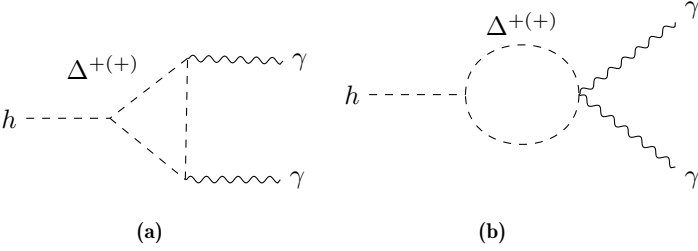


Figure 4: Feynman diagrams for the $h \to \gamma \gamma$ decay with charged scalars Δ^+ or Δ^{++} in the loop. The momenta assignments are identical to those in Figure 3.

5.1 Charged scalar contribution to $h \to \gamma \gamma$ decay width

To account for the effects of the hypothesized charged scalars, we evaluate the invariant amplitudes given by two additional Feynman diagrams, shown in Figure 4. The explicit computation is available in Appendix 8.1. When writing the total amplitude for the $h \to \gamma \gamma$ decay, $\mathcal{M}_{\text{SM+BSM}} = \mathcal{M}_{\text{SM}} + \mathcal{M}_{\text{BSM}}$, the factor F_{SM} defined in the previous section as (16) must be replaced with:

$$F_{\rm SM} \rightarrow F_{\rm SM+BSM} = F_{\rm SM} + \frac{C_{h\Delta\Delta}vQ_{\Delta}^2m_W}{m_{\Delta}^2g}F_{\Delta}, \qquad F_{\Delta} = \beta_{\Delta}\left(1 - \beta_{\Delta}f(\beta_{\Delta})\right), \qquad (20)$$

which now includes the contributions of a scalar particle with mass m_{Δ} and charge Q_{Δ} . The triple scalar coupling in the units of vev v is denoted by $C_{h\Delta\Delta}$.

5.2 Constraining the parameters of BSM models

The contributions of a singly or doubly charged scalar $\Delta^{+(+)}$ to $\Gamma_{h\to\gamma\gamma}$ depend on two parameters: the mass m_{Δ} and the dimensionless coupling $C_{h\Delta\Delta}$. Knowing the experimental values of observables, we can determine the constraints on these parameters.

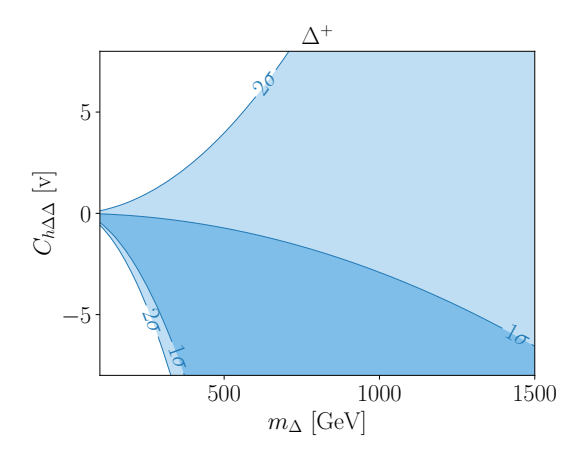
Signal strength μ is defined as the ratio of the observed events to the theoretical SM prediction. For the $h \to \gamma \gamma$ decay, the most recent experimental value is estimated at $\mu_{\rm exp} = 1.10 \pm 0.06$ [19]. We define the predicted signal strength accounting for the BSM effects, which were calculated earlier:

$$\mu_{\rm pred} = \frac{\Gamma_{\rm SM+BSM}}{\Gamma_{\rm SM}} \,. \tag{21}$$

Comparing it to μ_{exp} for various combinations of parameters m_{Δ} and $C_{h\Delta\Delta}$ using reduced χ^2 statistic, we obtain the constraints on the parameter space displayed in figure 5. The doubly charged scalar shows stronger constraints compared to the singly charged due to the Q_{Δ}^2 enhancement in (20). In both cases there is a preference towards negative couplings. It is important to emphasize that the apparent preference for nonzero $C_{h\Delta\Delta}$ does not exceed 1σ and therefore carries no statistical significance. Current ATLAS and CMS global fits of Higgs properties report diphoton signal strengths consistent with the SM within uncertainties [25]. As the mass of the hypothetical scalar increases, the constraints on the coupling loosen. Brief discussion on statistics as well as additional plots are available in the Phenomenology Appendix 8.2.

6 Conclusions

We demonstrated some of the essential features of the electroweak theory of the Standard model, with the key ingredient being the concept of the spontaneous breaking of the gauge symmetry – the Higgs mechanism – as the mathematical procedure which allows for the generation of the vector boson masses. The Higgs boson, predicted by the theory, decays to two photons through a loop-induced process with predominant contributions coming from the W boson and the top



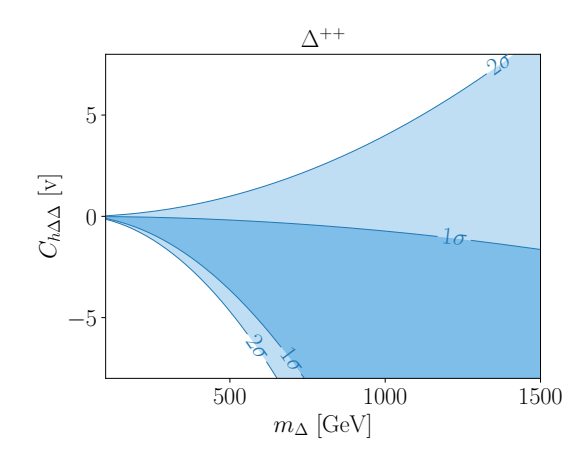


Figure 5: Likelihood of combinations of parameters for singly (left) and doubly charged (right) scalars with the darkest shaded area being the most likely. The contours represent the 1σ and 2σ confidence levels. Values outside the shaded regions can be considered excluded by experimental data.

quark. Although a rare decay, this channel presents a sensitive experimental probe into both the SM physics, as well as the potential BSM contributions.

We computed the SM prediction for the decay width and emended it by considering additional loop diagrams with arbitrary charged scalars. These arise in BSM models with extended Higgs sectors, such as the Type-II See-Saw, the LRSM and the MSSM. The loop calculations were performed using Package-X. The obtained results are in agreement with those found in the literature [21, 26].

Comparing the analytical expression for the signal strength of the $h \to \gamma \gamma$ decay width to its experimental value, we constrained the parameter space for the mass and the coupling of the hypothesized BSM Higgses. The results show a slight preference for negative couplings at 1σ statistical significance. This effect should not be interpreted as evidence of new physics. Rather, it illustrates the present experimental sensitivity of the diphoton channel to possible BSM contributions.

7 Theoretical appendices

Appendix A: Additional preliminaries

Here we provide some additional comments on the concepts introduced in the main part of this seminar, which the reader is assumed to be familiar with or are not crucial for the understanding of the subject, but can offer some informative insight.

Ad: Group representations.

- In the language of group theory, scalar, vector and fermion fields transform under different representations of the Lorentz group.
- The gauge fields are algebra-valued, which means they transform under the *adjoint representation* of the gauge group.

Chirality of fermions. Chirality is an intrinsic property of a particle, which is said to be either leftor right-handed, depending on its eigenvalue of the chirality operator. The latter is defined as the fifth Dirac γ matrix: $\gamma_5 = i\gamma_1\gamma_2\gamma_3\gamma_4$. For massless particles, chirality and helicity – projection of spin onto the direction of its momentum – coincide. A Dirac spinor ψ can be decomposed into its left- and right-handed components using projection operators P_L and P_R :

$$\psi = P_L \psi + P_R \psi \equiv \psi_L + \psi_R, \qquad P_{L,R} = \frac{1}{2} (\mathbb{1} \mp \gamma_5) .$$
(22)

Weak interaction and parity violation. Parity transformation is defined as the reflection of spatial coordinates: $\mathcal{P}: \vec{x} \to -\vec{x}, \quad t \to t$. Under parity transformation, chirality flips the sign. Unlike strong and electromagnetic interactions, processes induced by weak interactions are not symmetric under such transformation. Weak interaction therefore *violates parity* as it couples exclusively left-handed particles and right-handed antiparticles. Since neutrinos only interact weakly, hypothetical right-handed neutrinos have not (yet) been observed and are not considered in the SM.

Appendix B: Spontaneous breaking of a global symmetry

We will illustrate spontaneous breaking of a global symmetry with a concrete example. The following Lagrangian of n real scalar fields ϕ_i :

$$\mathcal{L} = \frac{1}{2} \partial_{\mu} \phi_{i} \partial^{\mu} \phi_{i} - V(\phi), \qquad V(\phi) = -\frac{1}{2} \mu^{2} (\phi_{i})^{2} + \frac{\lambda}{4} (\phi_{i})^{4}, \qquad i = 1, ..., n,$$
 (23)

is invariant under rotations among the fields ϕ_i : $\phi_i \to R_{ij}\phi_j$, $R^TR = 1$, and is therefore symmetric under the group of all orthogonal $n \times n$ matrices O(n), which has n(n-1)/2 generators. The potential $V(\phi)$ depends on two \mathbb{R} parameters: μ^2 and λ , where λ is taken to be positive in order to ensure a lower bound for the energies of the theory [27]. For $\mu^2 < 0$, the minimum of the potential is symmetric under rotations, which can be seen in Figure 6. For $\mu^2 > 0$, however, there are infinitely many degenerate vacua which do not remain invariant under O(n), allowing for SSB.

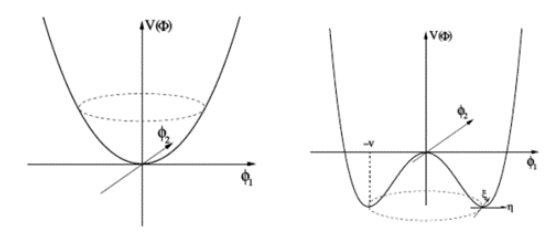


Figure 6: The shape of the potential V for $\mu^2 < 0$ (left) and for $\mu^2 > 0$ (right). Source: [28].

We choose one of the minima, for example $\phi_0 = (\phi_0^1, ..., \phi_0^N) = (0, ..., v)$, with $v = \mu/\sqrt{\lambda}$ as the vacuum expectation value (vev). Expanding the fields around it, we obtain:

$$\phi = (\pi_k(x), v + \sigma(x)), \qquad k = 1, ..., N - 1, \tag{24}$$

where π_k and σ are the perturbations around the vacuum. The Lagrangian (23) becomes:

$$\mathcal{L} = \frac{1}{2} \left(\partial_{\mu} \pi^{k} \right)^{2} + \frac{1}{2} \left(\partial_{\mu} \sigma \right)^{2} - \mu^{2} \sigma^{2} - \sqrt{\lambda} \mu \sigma^{3} - \sqrt{\lambda} \mu \left(\pi^{k} \right)^{2} \sigma - \frac{\lambda}{4} \sigma^{4} - \frac{\lambda}{2} \left(\pi^{k} \right)^{2} \sigma^{2} - \frac{\lambda}{4} \left(\pi^{k} \right)^{4}$$
, (25) and the initial $O(n)$ symmetry is no longer apparent. The Lagrangian is now invariant under the rotations among the π_{k} fields, which means the symmetry group has been broken down to $O(n-1)$. The number of broken generators corresponds to the difference in the number of symmetry generators before and after the SSB. In this case, this means: $n_{BG} = n(n-1)/2 - (n-1)(n-2)/2 = n-1$, which is precisely the number of the massless scalar fields π_{k} that appeared in the Lagrangian and are interpreted as the NGBs [12]. Notice that the σ field acquires a mass $m_{\sigma} = \sqrt{2}\mu$. It is also worth noting that in a Lorentz-invariant field theory, only scalar fields can have non-zero vevs, which is crucial for SSB.

What we have just shown was a spontaneous breaking of a global symmetry. When breaking a local symmetry, the procedure is very similar, with the main difference being in the implications of the resulting massless scalars. For a spontaneously broken local symmetry these would-be Goldstones are unphysical and become the longitudinal polarizations of the massive vector bosons [12].

Appendix C: Electroweak theory in the Standard model

The treatment of the electroweak theory in the main part of this article was limited to a rather conceptual description of its construction from group theoretical considerations and the subsequent procedure of the electroweak symmetry breaking. A more detailed analysis is available in the present section.

Masses of the weak bosons. By using the explicit definition of SU(2) generators in terms of Pauli matrices σ^a , the covariant derivative defined in (10) can be rewritten in a convenient matrix form:

$$\mathcal{D}_{\mu}\phi = \partial_{\mu}\phi + iG_{\mu}\phi, \qquad G_{\mu} = \frac{1}{2} \begin{pmatrix} gW_{\mu}^{3} + 2g'Y_{\phi}B_{\mu} & g(W_{\mu}^{1} - iW_{\mu}^{2}) \\ g(W_{\mu}^{1} + iW_{\mu}^{2}) & -gW_{\mu}^{3} + 2g'Y_{\phi}B_{\mu} \end{pmatrix}.$$
(26)

Knowing the mass terms are quadratic in gauge fields and are not coupled to any of the scalars, we extract them by investigating the following term:

$$(G_{\mu} \langle \phi \rangle)^{\dagger} (G^{\mu} \langle \phi \rangle), \quad \text{where} \quad G^{\mu} \langle \phi \rangle = \frac{v}{\sqrt{2}} \begin{pmatrix} \frac{1}{2} g \left(W_{\mu}^{1} - i W_{\mu}^{2} \right) \\ -\frac{1}{2} g W_{\mu}^{3} + g' Y_{\phi} B_{\mu} \end{pmatrix}, \tag{27}$$

which leads to:

$$(G_{\mu} \langle \phi \rangle)^{\dagger} (G^{\mu} \langle \phi \rangle) = \frac{1}{4} g^{2} v^{2} \frac{1}{\sqrt{2}} (W_{\mu}^{1} - iW_{\mu}^{2}) \frac{1}{\sqrt{2}} (W_{\mu}^{1} + iW_{\mu}^{2}) + \frac{1}{8} v^{2} (-gW_{\mu}^{3} + 2g'Y_{\phi}B_{\mu})^{2} . \quad (28)$$

Defining a linear combination $W_{\mu}^{\pm} = \frac{1}{\sqrt{2}} \left(W_{\mu}^{1} \mp i W_{\mu}^{2} \right)$ the first term becomes:

$$\frac{1}{4}g^2v^2W_{\mu}^+W^{-\mu} = \mathcal{L}_{W, \text{ mass}}, \qquad (29)$$

For a charged vector field, the factor of 1/2 in the normalization of the mass term in the Lagrangian defined in (1) is omitted, analogously to how a Lagrangian of a complex scalar field is defined. We therefore read off the mass of the W boson: $m_W = gv/2$. Finding the mass of the Z boson is slightly less straightforward. The key is to find two orthogonal linear combinations of real vector fields W^3_{μ} and B_{μ} for which the mass matrix is diagonal [16]. Computing the determinant of the mass matrix, we find:

$$M = \frac{1}{4}v^2 \begin{pmatrix} g^2 & -gg' \\ -gg' & g'^2 \end{pmatrix}, \quad \det M = 0 \qquad \rightarrow \qquad m_A^2 = 0, \quad m_Z^2 = \operatorname{Tr} M = \frac{1}{4}v^2(g^2 + g'^2). \quad (30)$$

Summary 7.1. The physical fields W_{μ}^{\pm}, Z_{μ} and A_{μ} – the photon field – can be written as linear combinations of the gauge fields we encountered in Equation (10):

•
$$W_{\mu}^{\pm} = \frac{1}{\sqrt{2}} \left(W_{\mu}^{1} \mp i W_{\mu}^{2} \right), \qquad m_{W} = \frac{1}{2} g v,$$

• $Z_{\mu} = \cos \theta_{W} W_{\mu}^{3} - \sin \theta_{W} B_{\mu}, \qquad m_{Z} = \frac{1}{2} \left(g^{2} + g'^{2} \right)^{1/2} v,$
• $A_{\mu} = \sin \theta_{W} W_{\mu}^{3} + \cos \theta_{W} B_{\mu}, \qquad m_{A} = 0.$ (31)

Here we introduced a new parameter – the weak mixing angle θ_W [16], defined as:

$$\tan \theta_W = \frac{g'}{g} \,. \tag{32}$$

The fields W_{μ}^{\pm} are complex and therefore charged, while Z_{μ} and A_{μ} are real, hence neutral. The photon remains massles after SSB, which is consistent with observations.

Mass of the Higgs boson. The mass of the Higgs boson is derived by investigating the Higgs potential given in (9) after the spontaneous symmetry breaking:

$$V(\phi) = -\mu^2 \phi^{\dagger} \phi + \lambda \left(\phi^{\dagger} \phi \right)^2, \qquad \phi = \begin{pmatrix} w_+ \\ \frac{1}{\sqrt{2}} \left(v + h + iz \right) \end{pmatrix}. \tag{33}$$

We want to isolate the terms that are quadratic in field h:

•
$$\phi^{\dagger} \phi = \frac{1}{2} (v+h)^2 + \dots = \frac{1}{2} h^2 + \dots$$

•
$$\left(\phi^{\dagger}\phi\right)^2 = \frac{1}{4}\left(v+h\right)^4 + \dots = \frac{1}{4}6v^2h^2 + \dots = \frac{3}{2}v^2h^2 + \dots$$

Putting it all together and keeping in mind that the parameters of the potential are related to the vev v through Equation (11), we get:

$$V(\phi) \supset \frac{1}{2} \left(3v^2 \lambda - \mu^2 \right) h^2 = \frac{1}{2} \left(3v^2 \lambda - \lambda v^2 \right) h^2 = \frac{1}{2} 2\lambda v^2 h^2 \quad \to \quad m_h = \sqrt{2\lambda} v \,.$$

Residual symmetry and the pattern of symmetry breaking. What exactly has happened to the symmetry group of the Lagrangian? The non-zero vev of the scalar doublet $\langle \phi \rangle$ has non-zero eigenvalues of the $\mathrm{SU}(2)_L$ generators, which means the latter are spontaneously broken as $T \langle \phi \rangle \neq 0$. The same goes for the $\mathrm{U}(1)_Y$ invariance. However, the photon is a gauge boson and it is massless, so there must be some residual $\mathrm{U}(1)$ symmetry after the SSB. Looking at the definition of A_μ in (31), we are inspired to construct a linear combination of T^3 and Y, called the electric charge Q:

$$Q = T^3 + Y, (34)$$

for which the lower component of the ϕ doublet has a zero eigenvalue, meaning the U(1)_Q symmetry is not broken by the vev of ϕ . This requirement fixes the hypercharge of the doublet. First we realize that the eigenvalue of the T^3 generator for the lower component of an SU(2) doublet is $t_3 = -1/2$. We find $Y_{\phi} = +1/2$ and note the electroweak symmetry group has been broken down to U(1)_Q:

$$SU(2)_L \otimes U(1)_Y \longrightarrow U(1)_Q$$
. (35)

The electroweak Lagrangian. We will discuss the terms relevant to the calculation of the $h \to \gamma \gamma$ decay, presented in Figure 7. The corresponding Feynman rules, which are summarized in 3.1, will not be derived explicitly. What follows is a brief outline of some of the key points.

The second term in (13) corresponds to the kinetic terms for the gauge fields. We know from Section 2.3 that these are of the form: $\mathcal{L}_{\text{gauge}}^{\text{pure}} = -\frac{1}{4}B_{\mu\nu}B^{\mu\nu} - \frac{1}{4}W_{\mu\nu}^aW_a^{\mu\nu}$, where

$$B_{\mu\nu} = \partial_{\mu}B_{\nu} - \partial_{\nu}B_{\mu}, \quad \text{and} \quad W_{\mu\nu}^{a} = \partial_{\mu}W_{\nu}^{a} - \partial_{\nu}W_{\mu}^{a} + g\varepsilon_{abc}W_{\mu}^{b}W_{\nu}^{c}.$$
 (36)

These fields first need to be mapped to the physical fields defined in (31). Their interactions can be derived from the terms that are cubic or quartic in the fields. For the propagators, we need to consider also the gauge boson mass terms in $\mathcal{L}_{\text{Higgs}}$. Moreover, because of the gauge invariance, the propagators cannot be defined unless we introduce the gauge-fixing terms [16] into the Lagrangian:

$$\mathcal{L}_{gf} = -\frac{1}{\xi_W} |\partial_\mu W_+^\mu + i\xi_W M_W w_+|^2 - \frac{1}{2\xi_Z} (\partial_\mu Z^\mu + \xi_Z M_Z z)^2 - \frac{1}{2\xi} (\partial_\mu A^\mu)^2,$$
 (37)

with ξ, ξ_W and ξ_Z as the arbitrary gauge parameters [16]. The propagators of the gauge and would-be-Goldstone bosons are then ξ -dependent. A possible choice of gauge is the *unitary gauge*, obtained by setting $\xi \to \infty$. In this limit, the propagators of the would-be-Goldstones vanish and the number of possible diagrams decreases significantly. For this reason, the calculation of the $h \to \gamma\gamma$ decay width was performed in the unitary gauge.

In addition to gauge-fixing terms, quantization of non-abelian gauge theories requires adding anticommuting scalar fields to the Lagrangian in the form of \mathcal{L}_{ghost} . These Fadeev-Popov ghosts are unphysical fields which are introduced through a mathematical procedure alongside \mathcal{L}_{gf} and restore unitarity of the S-matrix [12]. After SSB, they aquire a mass and their propagators are of the form:

$$Prop_{ghost} = \frac{i}{p^2 - \xi m^2},$$
(38)

which means in unitary gauge, they decouple and do not contribute to the amplitudes. A more detailed discussion on gauge-fixing and ghosts is available in [12].

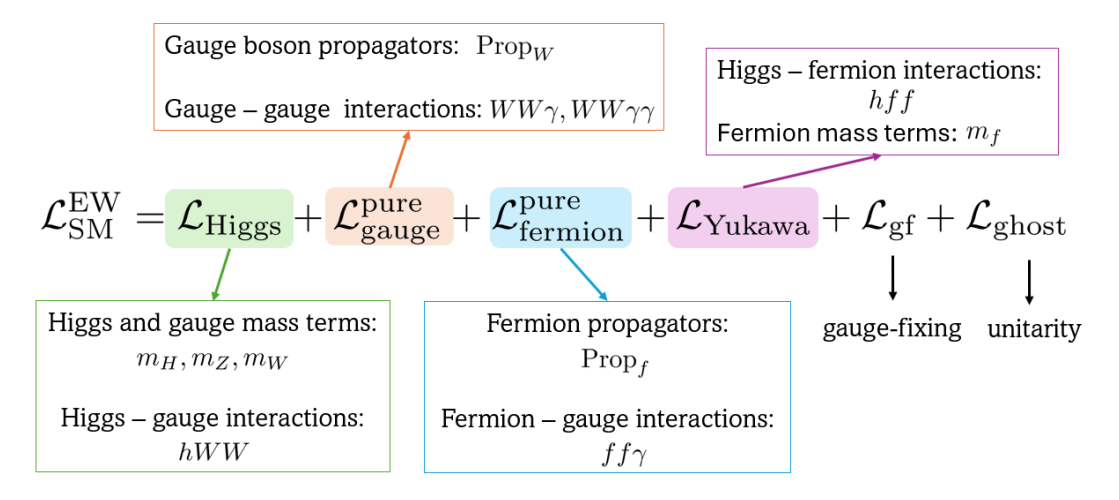


Figure 7: The structure of the electroweak Lagrangian.

The Yukawa sector describes the scalar-fermion interactions and after SSB includes the fermion mass terms. From the principles of gauge invariance we can construct the following [16]:

$$\mathcal{L}_{\text{Yukawa, leptons}} = -\sum_{l} \left(h_{l} \bar{\psi}_{l,L} \phi \, l_{R} + \text{h.c.} \right), \tag{39}$$

where $\psi_{l,L}$ is a SU(2) doublet of l-generation leptons with hypercharge Y = -1/2, ϕ is the scalar doublet introduced in (12) and l_R is an SU(2) singlet with Y = -1. It follows that both terms in (39) are SU(2)_L as well as U(1)_Y singlets. After SSB, we obtain the lepton masses: $m_l = h_l v / \sqrt{2}$ [16], as well as Higgs-lepton couplings. The introduction of quarks into $\mathcal{L}_{\text{Yukawa}}$ is analogous, although a bit more intricate, since there are two SU(2)_L singlets for each generation, e.g. u_R , d_R . Unlike right-handed neutrinos, right-handed down-type quarks are observed in the strong interactions.

The third term in the electroweak Lagrangian can be written as

$$\mathcal{L}_{\text{fermion, leptons}}^{\text{pure}} = \sum_{l} \left(\bar{\psi}_{l,L} i \gamma^{\mu} D_{\mu} \psi_{l,L} + \bar{l}_{R} i \gamma^{\mu} D_{\mu} l_{R} \right) \tag{40}$$

for leptons and similarly for quarks. The covariant derivatives are defined as:

$$D_{\mu}\psi_{l,L} = \left(\partial_{\mu} + ig\frac{\sigma^{a}}{2}W_{\mu}^{a} + ig'Y_{\psi}B_{\mu}\right)\psi_{l,L}, \qquad D_{\mu}l_{R} = \left(\partial_{\mu} + ig'Y_{l_{R}}B_{\mu}\right)l_{R}, \qquad (41)$$

where $Y_{\psi} = -1/2$ and $Y_{l_R} = -1$. This leads to the kinetic terms, which combined with the mass terms in $\mathcal{L}_{\text{Yukawa}}$ give the fermion propagators, as well as the fermion-gauge interactions.

7.1 Comments on higher-order renormalization

We mentioned in Section 4.2 that loop calculations generally lead to divergences, which need to be treated carefully in order to obtain finite results for the computed observables. This is achieved through *renormalization*.

Because there is no tree-level amplitude contributing to the diphoton decay of the Higgs boson and the theory is renormalizable, the process is already finite at 1-loop after considering all of the diagrams. Hence, beyond the usual regularization of loop integrals, no additional counterterms specific to this vertex are required. To illustrate the underlying workings of renormalization, we first consider a more general case.

We begin with a bare Lagrangian of the theory, \mathcal{L} , written in terms of the bare fields (ϕ_i) and parameters (α_i) , which are not yet renormalized. Loop diagrams evaluated using the Loop diagrams evaluated with the bare Feynman rules obtained from \mathcal{L} diverge in general. These infinities can be absorbed by introducing renormalized quantities: $\phi = Z_{\phi}^{1/2} \phi_R$, $\alpha = \mu^{\varepsilon} Z_{\alpha} \alpha$, and splitting the bare \mathcal{L} into a renormalized Lagrangian \mathcal{L}_R , and the counterterm Lagrangian, $\delta \mathcal{L}_{CT}$, containing divergences:

$$\mathcal{L}(\phi_i, \partial_\mu \phi_i; \alpha_i) \to \mathcal{L} = \mathcal{L}_{R}(\phi_i^R, \partial_\mu \phi_i^R; \alpha_i^R) + \delta \mathcal{L}_{CT}. \tag{42}$$

Here ϕ_i^R and α_i^R are the renormalized fields and parameters. From \mathcal{L}_R we extract the renormalized Feynman rules, while the counterterms in $\delta \mathcal{L}_{CT}$ are fixed by imposing renormalization conditions, depending on the chosen renormalization scheme. One common choice is the on-shell renormalization scheme, where the parameters are fixed to the experimental values of physical observables.

In general, an N-loop amplitude receives contributions from the genuine N-loop 1-particle-irreducible (1PI) diagrams, as well as from lower k-loop diagrams with counterterm insertions of total order m, such that k + m = N. This ensures that all UV divergences cancel order by order:

$$\mathcal{M}_{\text{ren}}^{(0)} = \mathcal{M}^{(\text{tree})},
\mathcal{M}_{\text{ren}}^{(1)} = \mathcal{M}_{1L}^{(1)} + \delta \mathcal{M}_{\text{CT}}^{(1)},
\mathcal{M}_{\text{ren}}^{(2)} = \mathcal{M}_{2L}^{(2)} + \mathcal{M}_{1L \oplus \delta^{(1)}}^{(2)} + \delta \mathcal{M}_{\text{CT}}^{(2)},
\mathcal{M}_{\text{ren}}^{(3)} = \mathcal{M}_{3L}^{(3)} + \mathcal{M}_{2L \oplus \delta^{(1)}}^{(3)} + \mathcal{M}_{1L \oplus \delta^{(2)}}^{(3)} + \delta \mathcal{M}_{\text{CT}}^{(3)}, \dots$$
(43)

with $\mathcal{M}_{\mathrm{NL}}^{(\mathrm{N})}$ denoting the genuine N-loop contributions, while the additional terms represent lower-order diagrams with counterterm insertions. If a tree amplitude $\mathcal{M}^{(\mathrm{tree})}$ exists, there is a contribution proportional to $\mathcal{M}^{(\mathrm{tree})}$ with order-N counterterms; otherwise this pure-CT term is absent.

Now, let's apply this to the calculation of the $h \to \gamma \gamma$ decay. In renormalizable theories (such as the SM), all counterterms are of the same form as operators already present in the Lagrangian. Due to the gauge structure, there is no tree-level $h\gamma\gamma$ vertex, and therefore no counterterm for it. Consequently, there is no CT insertion at 1-loop order. The divergences in the genuine 1-loop contributions cancel amongst themselves, which is a direct consequence of the gauge symmetry and renormalizability. At 1-loop, there is no need to compute any counterterms explicitly. Implicitly, we used the renormalized Feynman rules when evaluating the diagrams, with the parameters being renormalized rather than bare. A renormalization scheme must still be chosen for the input parameters, but the 1-loop UV finiteness is scheme-independent. Throughout the calculations we adopt the on-shell renormalization scheme: the parameters $(m_h, m_W, \alpha, g, ...)$ are identified with their physical, experimentally measured values.

At 2-loops, things would get more interesting. Besides the genuine 2-loop 1PI diagrams, one must also include (i) 1-loop diagrams with insertions of 1-loop counterterms in propagators or vertices, and (ii) external-leg field renormalizations multiplying the 1-loop amplitude. Still, since no tree-level $h\gamma\gamma$ operator exists in the SM, there is no pure counterterm diagram contributing directly to the vertex at any order.

8 Phenomenology appendices

8.1 Appendix A: Computation of $h \to \gamma \gamma$ decay width

Here we derive the results presented in Sections 4.2 and 5.1.

W loop. We begin by evaluating the invariant amplitude for the W loop. In unitary gauge, there are two Feynman diagrams contributing to this process, which are presented in Figure 3. The triangle diagram corresponds to the following amplitude:

$$i\mathcal{M}_{1} = 2 \int \frac{\mathrm{d}^{d}p}{(2\pi)^{d}} \left(igm_{W} g_{\alpha\beta} \right) \left(\frac{-i}{p^{2} - m_{W}^{2}} \left(g^{\alpha\gamma} - \frac{p^{\alpha}p^{\gamma}}{m_{W}^{2}} \right) \right)$$

$$\cdot \left(-ie \right) \left(g_{\gamma\lambda} \left(2p - k_{1} \right)_{\mu} + g_{\lambda\mu} \left(2k_{1} - p \right)_{\gamma} - g_{\mu\gamma} \left(k_{1} + p \right)_{\lambda} \right) \cdot \varepsilon^{\mu}(k_{1})$$

$$\cdot \left(\frac{-i}{(p - k_{1})^{2} - m_{W}^{2}} \left(g^{\lambda\rho} - \frac{(p - k_{1})^{\lambda}(p - k_{1})^{\rho}}{m_{W}^{2}} \right) \right)$$

$$\cdot \left(-ie \right) \left(g_{\rho\delta} \left(2p - 2k_{1} - k_{2} \right)_{\nu} + g_{\delta\nu} \left(2k_{2} + k_{1} - p \right)_{\rho} + g_{\nu\rho} \left(k_{1} - k_{2} - p \right)_{\delta} \right) \cdot \varepsilon^{\nu}(k_{2})$$

$$\cdot \left(\frac{-i}{(p - k_{1} - k_{2})^{2} - m_{W}^{2}} \left(g^{\beta\delta} - \frac{(p - k_{1} - k_{2})^{\beta}(p - k_{1} - k_{2})^{\delta}}{m_{W}^{2}} \right) \right) =$$

$$= 2 \int \frac{\mathrm{d}^{d}p}{(2\pi)^{d}} \frac{N_{\mu\nu}^{1}}{(p^{2} - m_{W}^{2}) \left((p - k_{1})^{2} - m_{W}^{2} \right) \left((p - k_{1} - k_{2})^{2} - m_{W}^{2}} \varepsilon^{\mu}(k_{1}) \varepsilon^{\nu}(k_{2}) .$$

$$(44)$$

Diagram 3a is symmetric under the interchange of the two gauge boson vertices, which is accounted for by having included a factor of 2 in (44) [21]. Next, we write down the amplitude for the bubble:

$$i\mathcal{M}_{2} = \int \frac{\mathrm{d}^{d} p}{(2\pi)^{d}} \left(igm_{W} g_{\alpha\beta} \right) \left(\frac{-i}{p^{2} - m_{W}^{2}} \left(g^{\alpha\gamma} - \frac{p^{\alpha} p^{\gamma}}{m_{W}^{2}} \right) \right)$$

$$\cdot \left(-ie^{2} \right) \left(2g_{\gamma\delta} g_{\mu\nu} - g_{\gamma\mu} g_{\delta\nu} - g_{\delta\mu} g_{\gamma\nu} \right) \cdot \varepsilon^{\mu} (k_{1}) \varepsilon^{\nu} (k_{2})$$

$$\cdot \left(\frac{-i}{(p - k_{1} - k_{2})^{2} - m_{W}^{2}} \left(g^{\beta\delta} - \frac{(p - k_{1} - k_{2})^{\beta} (p - k_{1} - k_{2})^{\delta}}{m_{W}^{2}} \right) \right)$$

$$= \int \frac{\mathrm{d}^{d} p}{(2\pi)^{d}} \frac{N_{\mu\nu}^{2}}{(p^{2} - m_{W}^{2}) \left((p - k_{1} - k_{2})^{2} - m_{W}^{2} \right)} \varepsilon^{\mu} (k_{1}) \varepsilon^{\nu} (k_{2}) .$$

$$(45)$$

We also note the on-shell conditions for initial and final states, as well as the Ward identities:

$$(k_1 + k_2)^2 = 2k_1 \cdot k_2 = m_h^2, \qquad k_1^2 = k_2^2 = 0, \qquad \varepsilon_\mu(k_1)k_1^\mu = \varepsilon_\nu(k_2)k_2^\nu. \tag{46}$$

Simplifying the two numerators $N_{\mu\nu}^{1,2}$ by hand requires a lot of error-prone algebra and performing the subsequent integration is anything but trivial. Alternatively, it is straightforward to use a Mathematica package suitable for loop calculations. The results below were computed with Package-X [20]. The corresponding Mathematica code is available in 2. For the total W boson-induced amplitude we get:

$$\mathcal{M}_{W} = \mathcal{M}_{1} + \mathcal{M}_{2} =$$

$$= \frac{e^{2}g}{(4\pi)^{2}m_{h}^{2}m_{W}} \left(m_{h}^{2} + 6m_{W}^{2} - 6m_{W}^{2} \left(m_{h}^{2} - 2m_{W}^{2} \right) C_{0}(0, 0, m_{h}^{2}, m_{W}^{2}, m_{W}^{2}, m_{W}^{2}) \right) \cdot \left(m_{h}^{2}g^{\mu\nu} - 2k_{2}^{\mu}k_{1}^{\nu} \right) \varepsilon_{\mu}(k_{1})\varepsilon_{\nu}(k_{2}),$$

$$(47)$$

which is in agreement with the result obtained in the 2012 paper by Marciano et al. [21]. In equation (47) we encounter a scalar Passarino-Veltman function C_0 , which is defined in [29] as

$$C_0(p_1^2, p_2^2, p^2, m_1^2, m_2^2, m_3^2) = 16\pi^2 i \int \frac{\mathrm{d}^d q}{(2\pi)^d} \frac{1}{(q^2 - m_1^2) \left((q + p_1)^2 - m_2^2 \right) \left((q + p_1 + p_2)^2 - m_3^2 \right)}$$
(48)

for $p + p_1 + p_2 = 0$ and can be evaluated analitically given the expression in the paper [21]:

$$C_0(m_h^2, 0, 0, m_W^2, m_W^2, m_W^2) = \frac{-2}{m_h^2} f\left(\frac{4m_W^2}{m_h^2}\right), \quad f(\beta) = \begin{cases} \arcsin^2\left(\beta^{-1/2}\right), & \beta \ge 1, \\ -\frac{1}{4}\left(\ln\frac{1+\sqrt{1-\beta}}{1-\sqrt{1-\beta}} - i\pi\right)^2, & \beta < 1. \end{cases}$$
(49)

Using (49) and defining $\beta_W = 4m_W^2/m_h^2$, we rewrite our W-loop amplitude as:

$$\mathcal{M}_W = \frac{e^2 g}{(4\pi)^2 m_W} \left(2 + 3\beta_W + 3 \left(2\beta_W - \beta_W^2 \right) f(\beta_W) \right) \left((k_1 \cdot k_2) g^{\mu\nu} - k_2^{\mu} k_1^{\nu} \right) \varepsilon_{\mu}(k_1) \varepsilon_{\nu}(k_2) \,. \tag{50}$$

Remark 8.1. When comparing the result (47) to (49), the following property of the Passarino-Veltman function C_0 was used: $C_0(0,0,m_h^2) = C_0(m_h^2,0,0)$, which holds if all of the propagator poles are equal. In general, C_0 is symmetric under cyclic permutations of its arguments.

The individual integrals corresponding to the triangle (\mathcal{M}_1) and bubble (\mathcal{M}_2) diagrams contain divergences when evaluated in dimensional regularization. However, these divergences cancel exactly in the sum, so that the total W-boson contribution \mathcal{M}_W is finite.

Fermion loop. There is only one diagram for the fermion loop, see Figure 3c. It is symmetric under the interchange of the two photons, which again yields a factor of two. Since we are dealing with a closed fermion loop, we take the trace of the propagators and vertices and include a factor of -1 [12]. The corresponding invariant amplitude is then:

$$i\mathcal{M}_{f} = 2 \int \frac{\mathrm{d}^{n} p}{(2\pi)^{n}} N_{f}(-1) \operatorname{Tr} \left[\left(-i \frac{g}{2} \frac{m_{f}}{m_{W}} \right) \frac{i \left(\not p + m_{f} \right)}{p^{2} - m_{f}^{2}} \left(-i e Q_{f} \gamma_{\mu} \right) \right. \\ \left. \times \frac{i \left(\not p - \not k_{1} + m_{f} \right)}{(p - k_{1})^{2} - m_{f}^{2}} \left(-i e Q_{f} \gamma_{\nu} \right) \frac{i \left(\not p - \not k_{1} - \not k_{2} + m_{f} \right)}{(p - k_{1} - k_{2})^{2} - m_{f}^{2}} \right] \varepsilon_{\mu}(k_{1}) \varepsilon_{\nu}(k_{2})$$

$$= 2 \int \frac{\mathrm{d}^{n} p}{(2\pi)^{n}} \frac{N_{\mu\nu}^{f}}{\left(p^{2} - m_{f}^{2} \right) \left((p - k_{1})^{2} - m_{f}^{2} \right) \left((p - k_{1} - k_{2})^{2} - m_{f}^{2} \right)} \varepsilon_{\mu}(k_{1}) \varepsilon_{\nu}(k_{2}) ,$$

$$(51)$$

where Q_f is the electric charge of the fermion in units of e and N_f is the color factor, which is 1 for leptons and 3 for quarks. The on-shell conditions and the Ward identities are the same as defined in (46). The result was again computed using Package-X (see 3) and is the following:

$$\mathcal{M}_{f} = \frac{Q_{f}^{2} e^{2} g N_{f}}{(4\pi)^{2} m_{W}} \frac{m_{f}^{2}}{m_{h}^{2}} \left(-2 + \left(m_{h}^{2} - 4m_{f}^{2} \right) C_{0}(0, 0, m_{h}^{2}, m_{f}^{2}, m_{f}^{2}, m_{f}^{2}, m_{f}^{2}) \right) \cdot \left(m_{h}^{2} g^{\mu\nu} - 2k_{1}^{\nu} k_{2}^{\mu} \right) \varepsilon_{\mu}(k_{1}) \varepsilon_{\nu}(k_{2})$$

$$= \frac{e^{2} g}{(4\pi)^{2} m_{W}} N_{f} Q_{f}^{2} \left(-2\beta_{f} \left(1 + (1 - \beta_{f}) f(\beta_{f}) \right) \right) \left(k_{1} \cdot k_{2} g^{\mu\nu} - k_{1}^{\nu} k_{2}^{\mu} \right) \varepsilon_{\mu}(k_{1}) \varepsilon_{\nu}(k_{2}) ,$$

$$(52)$$

where we defined $\beta_f = 4m_f^2/m_h^2$. This amplitude is finite.

Scalar loop. When considering BSM models with charged scalars, two additional diagrams, shown in Figure 4, contribute to the total amplitude. The Feynman rules are in principle model-dependent, however the overall vertex and propagator structure can be generalized by considering arbitrary couplings and masses. The rules can therefore be deduced from the MSSM Lagrangian or found in the paper [26]. We denote the triple scalar coupling in the units of vev v by $C_{h\Delta\Delta}$ and write the amplitudes for the two diagrams:

$$i\mathcal{M}_{a} = 2 \int \frac{\mathrm{d}^{n} p}{(2\pi)^{n}} \left(-iC_{h\Delta\Delta}v\right) \frac{i}{p^{2} - m_{\Delta}^{2}} \left(-iQ_{\Delta}e(2p - k_{1})_{\mu}\right) \frac{i}{(p - k_{1})^{2} - m_{\Delta}^{2}} \cdot \left(-iQ_{\Delta}e(2p - 2k_{1} - k_{2})_{\nu}\right) \frac{i}{(p - k_{1} - k_{2})^{2} - m_{\Delta}^{2}} \cdot \varepsilon^{\mu}(k_{1})\varepsilon^{\nu}(k_{2}),$$

$$(53)$$

$$i\mathcal{M}_{b} = \int \frac{\mathrm{d}^{n} p}{(2\pi)^{n}} \left(-iC_{h\Delta\Delta}v\right) \frac{i}{p^{2} - m_{\Delta}^{2}} \left(2iQ_{\Delta}^{2}e^{2}g_{\mu\nu}\right) \frac{i}{(p - k_{1} - k_{2})^{2} - m_{\Delta}^{2}} \cdot \varepsilon^{\mu}(k_{1})\varepsilon^{\nu}(k_{2}). \tag{54}$$

Here m_{Δ} and Q_{Δ} correspond to the mass and the charge of $\Delta^{+(+)}$. The factor of 2 in Equation (53) accounts for the symmetry of the first diagram. Using Package-X (see Appendix 8.1) and imposing the conditions specified in (46) we obtain the finite scalar contribution to the amplitude:

$$\mathcal{M}_{\text{BSM}} = \mathcal{M}_a + \mathcal{M}_b = \frac{2C_{h\Delta\Delta}vQ_{\Delta}^2e^2}{(4\pi)^2m_h^2} \left(m_{\Delta}^2g_{\mu\nu} - 2k_{1\nu}k_{2\mu}\right) + \left(1 + 2m_{\Delta}^2C_0(0, 0, m_h^2, m_{\Delta}^2, m_{\Delta}^2, m_{\Delta}^2)\right)\varepsilon^{\mu}(k_1)\varepsilon^{\nu}(k_2),$$
(55)

which can be rewritten as:

$$\mathcal{M}_{\text{BSM}} = \frac{C_{h\Delta\Delta}vQ_{\Delta}^2e^2}{(4\pi)^2m_{\Delta}^2}\beta_{\Delta}\left(1 - \beta_{\Delta}f(\beta_{\Delta})\right)\left((k_1 \cdot k_2)g_{\mu\nu} - k_{1\nu}k_{2\mu}\right) \cdot \varepsilon^{\mu}(k_1)\varepsilon^{\nu}(k_2), \quad \beta_{\Delta} = \frac{4m_{\Delta}^2}{m_{L}^2}. \quad (56)$$

```
In[1]:= << "X"
       Package-X v2.1.1, by Hiren H. Patel
       For more information, see the guide
ln[2]:= onshell = {k1.k1 \rightarrow 0, k2.k2 \rightarrow 0, k1.k2 \rightarrow mh^2 / 2}
       ward = \{k1_{\mu} \rightarrow 0, k2_{\nu} \rightarrow 0\}
In[4]:= diagramScalar1 =
        LoopIntegrate [(-I ChDD v) I (-IQe (2p - k1)_u) I (-IQe (2p - 2k1 - k2)_v) I,
              p, {p, mH}, {p-k1, mH}, {p-k1-k2, mH},
              Cancel → True] /. onshell /. ward // FullSimplify
Out[4] = 4 ChDD e^2 Q^2 v
         PVC[0, 1, 1, 0, 0, mh^2, mH, mH, mH]) + g_{\mu,\nu} PVC[1, 0, 0, 0, 0, mh^2, mH, mH, mH])
In[6]:= diagramScalar2 =
        LoopIntegrate[(-I ChDD v) I (2 I e^2 Q^2 g_{\mu,\nu}) I, p, {p, mH}, {p - k1 - k2, mH},
              Cancel → True] /. onshell /. ward // FullSimplify
Out[6]= -2 \text{ ChDD } e^2 Q^2 \vee g_{\mu,\nu} \text{ PVB} [0, 0, \text{mh}^2, \text{mH}, \text{mH}]
In[7]:= bothDiagramsScalar = 2 diagramScalar1 + diagramScalar2
In[8]:= LoopRefine[bothDiagramsScalar, Part → UVDivergent]
Out[8]= 0
In[9]:= LoopRefine[bothDiagramsScalar, ExplicitC0 → None] // DiscExpand // FullSimplify
       2~\text{ChDD}~e^2~Q^2~v~\left(-2~\text{k1}_{\scriptscriptstyle V}~\text{k2}_{\scriptscriptstyle \mu} + \text{mh}^2~\text{g}_{\scriptscriptstyle \mu,\scriptscriptstyle V}\right)~\left(1 + 2~\text{mH}^2~\text{ScalarCO}\left[\textrm{0, 0, mh}^2\textrm{, mH, mH, mH}\right]\right)
```

Mathematica Code 1: Computation of the scalar loop amplitude.

Remark 8.2. It is important to note that when using Package-X for evaluating loop integrals, an overall factor of $i/(4\pi)^2$ is omitted from the displayed final results. Furthermore, the combination of terms $1/\varepsilon - \gamma_E + \log(4\pi)$ which arises after the dimensional regularization of divergent integrals is abbreviated to $1/\tilde{\varepsilon}$ [30].

```
In[1]:= << "X"
                  Package-X v2.1.1, by Hiren H. Patel
                  For more information, see the guide
  ln[2]:= onshell = {k1.k1 \rightarrow 0, k2.k2 \rightarrow 0, k1.k2 \rightarrow mh^2 / 2}
                  ward = \{k1_{\mu} \rightarrow 0, k2_{\nu} \rightarrow 0\}
  In[4]:= Wnumerator1 =
                      Contract[(I) \ g_{\alpha,\beta} \ (-I) \ (g_{\alpha,\phi} - p_{\alpha} \ p_{\phi} \ / \ mW^2) \ (-I) \ (g_{\phi,\lambda} \ (2 \ p - k1)_{\mu} + g_{\lambda,\mu} \ (2 \ k1 - p)_{\phi} - g_{\mu,\mu} \ (2 \ k1 - p)_{\phi} - g_{\mu,\mu} \ (2 \ k1 - p)_{\phi} \ (-1) \ (g_{\phi,\lambda} \ (2 \ p - k1)_{\mu} + g_{\lambda,\mu} \ (2 \ k1 - p)_{\phi} - g_{\mu,\mu} \ (-1) \ (g_{\mu,\lambda} \ (2 \ p - k1)_{\mu} + g_{\lambda,\mu} \ (-1)_{\mu} + g_{\lambda,\mu} \ (-1)_{\phi} - g_{\mu,\mu} \ (-1)_{\phi} \ (
                                               g_{\mu,\phi} (k1+p)_{\lambda} (-I) (g_{\lambda,\rho}-(p-k1)_{\lambda}(p-k1)_{\rho}/mW^2) (-I)
                                         (g_{\rho,\delta} (2p-2k1-k2)_{\nu} + g_{\delta,\nu} (2k2+k1-p)_{\rho} + g_{\nu,\rho} (k1-k2-p)_{\delta}) (-I)
                                         (g_{\beta,\delta}-(p-k1-k2)_{\beta}(p-k1-k2)_{\delta}/mW^2)] /. onshell /. ward // FullSimplify
  In[5]:= Wnumerator2 =
                      \mathsf{Contract}[\,(\mathbf{I})\ g_{\alpha,\beta}\ (-\,\mathbf{I})\ (g_{\alpha,\phi}-p_{\alpha}\ p_{\phi}\ /\ \mathsf{mW}^{\,\mathbf{\Delta}}2)\ (-\,\mathbf{I})\ (2\,g_{\phi,\delta}\,g_{\mu,\nu}-g_{\phi,\mu}\,g_{\delta,\nu}-g_{\delta,\mu}\,g_{\phi,\nu})\ (-\,\mathbf{I})
                                         (g_{\delta,\beta}-(p-k1-k2)_{\delta}(p-k1-k2)_{\beta}/mW^2)] /. onshell /. ward // FullSimplify
  ln[6]:= Wdiagram1 = LoopIntegrate[Wnumerator1, p, {p, mW}, {p - k1, mW},
                                     \{p - k1 - k2, mW\}, Cancel \rightarrow True\} /. onshell /. ward // FullSimplify
  In[7]:= Wdiagram2 =
                      LoopIntegrate[Wnumerator2, p, {p, mW}, {p - k1 - k2, mW}, Cancel → True] /. onshell /.
                             ward // FullSimplify
  In[8]:= Wbothdiagrams = (2 Wdiagram1 + Wdiagram2) // FullSimplify
 Out[8]= \frac{1}{2 \text{ mW}^4} \left( 8 \text{ mW}^2 \text{ k1}_{V} \text{ k2}_{\mu} \left( 4 \text{ mW}^2 \text{ PVC} \left[ 0, 0, 0, 0, 0, \text{mh}^2, \text{mW}, \text{mW}, \text{mW} \right] + \right) \right)
                                     (mh^2 + 2 (-1 + d) mW^2) (PVC[0, 0, 1, 0, 0, mh^2, mW, mW, mW] +
                                               PVC[0, 0, 2, 0, 0, mh^2, mW, mW] + PVC[0, 1, 1, 0, 0, mh^2, mW, mW, mW])) +
                         \mathbb{G}_{\mu,\vee} \left(-\text{mW}^2\text{ PVA}[0,\text{mW}] + d\text{ PVA}[1,\text{mW}] - \text{mh}^4\text{ PVB}[0,0,\text{mh}^2,\text{mW},\text{mW}] - \text{mW}^4\text{ PVA}[0,\text{mW}]\right)
                                    2 (2 \text{ mW}^2 (\text{mh}^2 + (-1 + d) \text{ mW}^2) \text{ PVB} [0, 0, \text{mh}^2, \text{mW}, \text{mW}] + \text{mh}^2
                                                   ((mh^2 + 2 mW^2) PVB[0, 1, mh^2, mW, mW] + 8 mW^4 PVC[0, 0, 0, 0, 0, mh^2, mW, mW, mW])) + 8 mW^4 PVC[0, 0, 0, 0, 0, mh^2, mW, mW, mW]))
                                    8 \text{ mW}^2 \left( \text{mh}^2 + 2 \left( -1 + d \right) \text{ mW}^2 \right) \text{ PVC} \left[ 1, 0, 0, 0, 0, \text{mh}^2, \text{mW}, \text{mW}, \text{mW} \right] \right)
  In[9]:= LoopRefine[Wbothdiagrams, Part → UVDivergent]
 Out[9]= 0
In[10]:= LoopRefine[Wbothdiagrams, ExplicitC0 → None] // DiscExpand // FullSimplify
                     (2 k1_{V} k2_{U} - mh^{2} g_{U,V}) (-mh^{2} - 6 mW^{2} + 6 mW^{2} (mh^{2} - 2 mW^{2}) Scalarco[0, 0, mh^{2}, mW, mW, mW])
                                                                                                                                           mh^2 mW^2
```

Mathematica Code 2: Notebook with evaluated amplitude for the W loop.

Remark 8.3. In the case of copying any of the provided code into Mathematica, subscripted indices will not be treated properly due to the limitations of Mathematica code listing in LaTeX. Subscripts should therefore be inserted manually.

```
In[1]:= << "X"
       Package-X v2.1.1, by Hiren H. Patel
       For more information, see the guide
ln[2]:= onshell = {k1.k1 \rightarrow 0, k2.k2 \rightarrow 0, k1.k2 \rightarrow mh^2 / 2}
       ward = \{k1_{\mu} \rightarrow 0, k2_{\nu} \rightarrow 0\}
ln[4]:= FNumerator = 2 Spur[(-I) I (p.\gamma + mf1), (-I \gamma_{\mu}),
              I (p.\gamma - k1.\gamma + mf1), (-I\gamma\gamma), I (p.\gamma - k1.\gamma - k2.\gamma + mf1)] // FullSimplify
Out[4] = 8 \text{ mf } (k1_{V} (k2_{\mu} - 4 p_{\mu}) - 2 p_{\mu} (k2_{V} - 2 p_{V}) +
            k1_{\mu} (2 k1_{\nu} + k2_{\nu} - 2 p_{\nu}) + (mf<sup>2</sup> - k1.k1 - k1.k2 + 2 k1.p - p.p) g_{\mu,\nu})
In[5]:= Fdiagram = LoopIntegrate[FNumerator, p, {p, mf}, {p-k1, mf},
                {p - k1 - k2, mf}, Cancel → True] /. onshell /. ward // FullSimplify
Out[5]= 8 mf k1_{\nu} k2_{\mu}
           0, 2, 0, 0, mh^2, mf, mf, mf] + PVC[0, 1, 1, 0, 0, mh^2, mf, mf, mf])) -
         4 mf g_{\mu,\nu} (2 PVB \left[0,0,\text{mh}^2,\text{mf},\text{mf}\right] + mh^2 PVC \left[0,0,0,0,\text{mh}^2,\text{mf},\text{mf},\text{mf}\right] -
             8 PVC [1, 0, 0, 0, 0, mh<sup>2</sup>, mf, mf, mf])
In[6]:= LoopRefine[Fdiagram, Part → UVDivergent]
Out[6]= 0
In[7]:= LoopRefine[Fdiagram, ExplicitC0 → None] // DiscExpand // FullSimplify
        \frac{4\,\text{mf}\,\left(2\,\text{k1}_{\text{\tiny V}}\,\text{k2}_{\mu}-\text{mh}^2\,\mathbb{g}_{\mu,\text{\tiny V}}\right)\,\left(-\,2\,+\,\left(-\,4\,\text{mf}^2\,+\,\text{mh}^2\right)\,\text{ScalarCO}\!\left[\,\text{0, 0, mh}^2\,,\,\text{mf, mf, mf}\,\right]\,\right)}{}
```

Mathematica Code 3: Mathematica notebook for the fermion loop.

Decay width. We wish to calculate the decay width for an unpolarized two-body decay given by:

$$\Gamma_{A\to 12} = \frac{|\vec{p}_f|}{32\pi^2 m_A^2} \int |\overline{\mathcal{M}}|^2 d\Omega.$$
 (57)

First, we recall the expression for the invariant amplitude (15) and compute its complex conjugate:

•
$$\mathcal{M} = \frac{e^2 g}{(4\pi)^2 m_W} F\left(k_1 \cdot k_2 g^{\mu\nu} - k_1^{\nu} k_2^{\mu}\right) \varepsilon_{\mu}(k_1) \varepsilon_{\nu}(k_2)$$

• $\mathcal{M}^* = \frac{e^2 g}{(4\pi)^2 m_W} F^* \left(k_1 \cdot k_2 g^{\rho\sigma} - k_1^{\sigma} k_2^{\rho}\right) \varepsilon_{\rho}^*(k_1) \varepsilon_{\sigma}^*(k_2)$, (58)

which leads to the squared amplitude averaged over all photon polarizations:

$$|\overline{\mathcal{M}}|^{2} = \frac{e^{4}g^{2}}{(4\pi)^{4}m_{W}^{2}}|F|^{2} \left(\frac{m_{h}^{2}}{2}g^{\mu\nu} - k_{2}^{\mu}k_{1}^{\nu}\right) \left(\frac{m_{h}^{2}}{2}g^{\rho\sigma} - k_{2}^{\rho}k_{1}^{\sigma}\right) \sum_{pol} \varepsilon_{\rho}^{*}(k_{1})\varepsilon_{\mu}(k_{1}) \sum_{pol} \varepsilon_{\sigma}^{*}(k_{2})\varepsilon_{\nu}(k_{2}).$$
(59)

Here we recalled the on-shell relation $k_1 \cdot k_2 = m_h^2/2$. We can replace the sums over external photons:

$$\sum_{pol.} \varepsilon_{\mu}^* \varepsilon_{\nu} \to -g_{\mu\nu} \,, \tag{60}$$

which after expressing the prefactor in terms of the Fermi and fine-structure constants leads to

$$|\overline{\mathcal{M}}|^{2} = |F|^{2} \left(\frac{\alpha}{4\pi}\right)^{2} \frac{8G_{F}}{\sqrt{2}} \left(\frac{m_{h}^{2}}{2} g^{\mu\nu} - k_{2}^{\mu} k_{1}^{\nu}\right) \left(\frac{m_{h}^{2}}{2} g^{\rho\sigma} - k_{2}^{\rho} k_{1}^{\sigma}\right) (-g_{\rho\mu}) (-g_{\sigma\nu}) =$$

$$= |F|^{2} \left(\frac{\alpha}{4\pi}\right)^{2} \frac{8G_{F}}{\sqrt{2}} \left(\frac{m_{h}^{4}}{4} - \frac{m_{h}^{2}}{2} 2k_{1} \cdot k_{2} + k_{1}^{2} k_{2}^{2}\right) =$$

$$= |F|^{2} \left(\frac{\alpha}{4\pi}\right)^{2} \frac{8G_{F}}{\sqrt{2}} \frac{m_{h}^{4}}{2} = |F|^{2} \left(\frac{\alpha}{4\pi}\right)^{2} \frac{4G_{F}}{\sqrt{2}} m_{h}^{4}.$$
(61)

Now we can use equation (57) to calculate the decay width. Since the squared amplitude has no angular dependance, it is trivial to integrate it over the solid angle:

$$\int d\Omega |\overline{\mathcal{M}}|^2 = |\overline{\mathcal{M}}|^2 \frac{1}{2} \cdot 4\pi.$$
 (62)

We need to be careful to include a factor of 1/2 which arises due to the fact that the two final states are identical. The integration limits are therefore

$$\int_0^{\pi/2} d\theta \int_0^{2\pi} d\phi \quad \text{and not} \quad \int_0^{\pi} d\theta \int_0^{2\pi} d\phi.$$
 (63)

Hence we get:

$$\Gamma_{h \to \gamma \gamma} = \frac{|\vec{p}_{\gamma}|}{32\pi^2 m_h^2} 2\pi |\overline{\mathcal{M}}|^2. \tag{64}$$

Lastly, the magnitude of the massless final state momentum $|\vec{p}_{\gamma}|$ can be expressed in the center-of-mass system as $|\vec{p}_{\gamma}| = m_h/2$. We arrive at the final result:

$$\Gamma_{h \to \gamma \gamma} = \frac{m_h^3 G_F}{8\sqrt{2}\pi} \left(\frac{\alpha}{4\pi}\right)^2 |F|^2. \tag{65}$$

8.2 Appendix B: Finding the parameter constraints

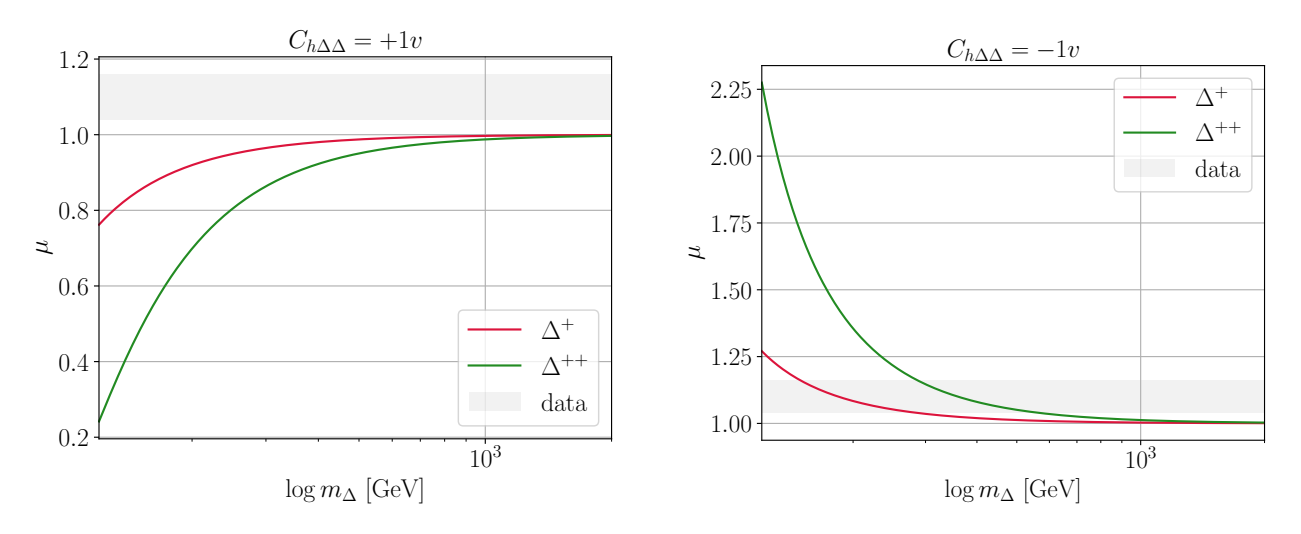


Figure 8: Predicted signal strengths at different values of mass m_{Δ} in the case of positive (+1) and negative (-1) coupling for the singly and doubly charged scalars. The gray shaded area represents the experimental value.

The parameters were constrained by evaluating the following function for the each set of parameters:

$$\chi^{2}(m_{\Delta}, C_{h\Delta\Delta}) = \left(\frac{\mathcal{O}_{\exp} - \mathcal{O}_{\operatorname{pred}}(m_{\Delta}, C_{h\Delta\Delta})}{\sigma}\right)^{2}, \tag{66}$$

where \mathcal{O}_{exp} and $\mathcal{O}_{\text{pred}}$ are the measured and the predicted values of an observable and σ is the experimental uncertainty. Expression (66) corresponds to the reduced χ^2 statistic, which is used in goodness-of-fit testing. The lower the value of χ^2 , the better the fit. For a two-parameter fit like in our case, 1σ confidence level (68.3% probability) equals to $\chi^2 = 2.30$. This means that for the sets of parameters in the darker shaded regions in figure 5, the value of χ^2 is lower than that.

Some helpful insight into the behaviour of BSM corrections can be gained by examining Figure 8. As the mass increases, BSM effects become negligeable for these values of the coupling. Again, negative coupling seems to be in better agreement with the data.

REFERENCES

- [1] P. Higgs, Broken Symmetries and the Masses of Gauge Bosons, Phys. Rev. Lett. 13 (1964), 508-509.
- [2] F. Englert and R. Brout, Broken Symmetry and the Mass of Gauge Vector Mesons, Phys. Rev. Lett. 13 (1964), 321–323.
- [3] G. S. Guralnik, C. R. Hagen, and T. W. B. Kibble, Global Conservation Laws and Massless Particles, Phys. Rev. Lett. 13 (1964), 585-587.
- [4] S. Weinberg, A Model of Leptons, Phys. Rev. Lett. 19 (1967), 1264–1266.
- [5] A. Salam, Weak and Electromagnetic Interactions, Conf. Proc. C 680519 (1968), 367–377.
- [6] S. L. Glashow, Partial Symmetries of Weak Interactions, Nucl. Phys. 22 (1961), 579–588.
- [7] G. 't Hooft and M. Veltman, Regularization and renormalization of gauge fields, Nuclear Physics B 44 (1972), no. 1, 189–213.
- [8] G. Aad et al., Observation of a new particle in the search for the Standard Model Higgs boson with the ATLAS detector at the LHC, Phys. Lett. B 716 (2012), 1–29.
- [9] S. Chatrchyan et al., Observation of a New Boson at a Mass of 125 GeV with the CMS Experiment at the LHC, Phys. Lett. B 716 (2012), 30-61.
- [10] K. Schmitz, Physical Chemistry: Multidisciplinary Applications in Society, Elsevier, 2016.
- [11] A. Tumasyan et al., A portrait of the Higgs boson by the CMS experiment ten years after the discovery., Nature 607 (2022), no. 7917, 60–68, [Erratum: Nature 623, (2023)].
- [12] M. E. Peskin and D. V. Schroeder, An Introduction to quantum field theory, Addison-Wesley, Reading, USA, 1995.
- [13] R. N. Mohapatra and P. B. Pal, Massive neutrinos in physics and astrophysics. Second edition, vol. 60, 1998.
- [14] T. Cheng and L. Li, Gauge Theory of Elementary Particle Physics, Oxford University Press, Oxford, UK, 1984.
- [15] J. Goldstone, A. Salam, and S. Weinberg, Broken symmetries, Phys. Rev. 127 (1962), 965–970.
- [16] P. B. Pal, An Introductory Course of Particle Physics, CRC Press, 7 2014.
- [17] J. C. Romao and J. P. Silva., A resource for signs and Feynman diagrams of the Standard Model, Int. J. Mod. Phys. A 27 (2012), 1230025.
- [18] G. Aad et al., Measurement of the Higgs boson mass with H→γγ decays in 140 fb−1 of s=13 TeV pp collisions with the ATLAS detector, Phys. Lett. B 847 (2023), 138315.
- [19] S. Navas et al., Review of particle physics, Phys. Rev. D 110 (2024), no. 3, 030001.
- [20] H. H. Patel, Package -x 2.0: A mathematica package for the analytic calculation of one-loop integrals, Computer Physics Communications 218 (2017), 66–70.
- [21] W. J. Marciano, C. Zhang, and S. Willenbrock, Higgs decay to two photons, Physical Review D 85 (2012), no. 1.
- [22] R. N. Mohapatra and G. Senjanovic, Neutrino Mass and Spontaneous Parity Nonconservation, Phys. Rev. Lett. 44 (1980), 912.
- [23] R. N. Mohapatra and J. C. Pati, A Natural Left-Right Symmetry, Phys. Rev. D 11 (1975), 2558.
- [24] S. Dimopoulos and H. Georgi, Softly Broken Supersymmetry and SU(5), Nucl. Phys. B 193 (1981), 150–162.
- [25] A. Tumasyan, W. Adam, J. W. Andrejkovic, T. Bergauer, S. Chatterjee, K. Damanakis, M. Dragicevic, A. Escalante Del Valle, P. S. Hussain, M. Jeitler, N. Krammer, L. Lechner, D. Liko, I. Mikulec, P. Paulitsch, F. M. Pitters, J. Schieck, R. Schöfbeck, D. Schwarz, S. Templ, W. Waltenberger, C.-E. Wulz, M. R. Darwish, and T. Janssen, A portrait of the higgs boson by the cms experiment ten years after the discovery, Nature 607 (2022), no. 7917, 60–68.
- [26] A. Djouadi, The anatomy of electroweak symmetry breaking tome ii: The higgs bosons in the minimal supersymmetric model, Physics Reports 459 (2008), no. 1–6, 1–241.
- [27] A. Djouadi, The anatomy of electroweak symmetry breaking, Physics Reports 457 (2008), no. 1-4, 1-216.
- [28] Ö. Özdal, The higgs boson and right-handed neutrinos in supersymmetric models, Ph.D. thesis, 07 2016.
- [29] H. Haber, One-loop qcd correction to the $\gamma^* q\bar{q}$ vertex, 1999.
- [30] V. Shtabovenko, FeynHelpers: Connecting FeynCalc to FIRE and Package-X, Comput. Phys. Commun. 218 (2017), 48–65.